Applications of Bayesian Data Analysis in KSTAR

Jaewook Kim,
and on behalf of KSTAR Team and collaborators

Korea Institute of Fusion Energy, Daejeon, Korea

E-mail: ijwkim@kfe.re.kr

Contents

- Introduciton to Bayesian inference
  - Bayes' theorem
  - TS & TCI data fusion for density profile estimation
- Practical use of Bayesian inference in KSTAR
  - Data fusion for plasma edge density profile refinement with BES
  - Data fusion of magnetic coil and Hall effect sensor
  - Gaussian process tomography with nonnegative prior
- Summary

Bayesian inference

$$P(H|D) = \frac{P(D|H)P(H)}{P(D)}$$

- $P(H|D)$: Posterior
  - The probability that the hypothesis is true with given measured data (Inference)
- $P(D|H)$: Likelihood
  - The probability that the data is generated with given hypothesis
- $P(H)$: Prior
  - The probability that the hypothesis is true
- $P(D)$: Evidence or Marginal likelihood

$P(H)$ can be

- Gaussian process to model smooth spatial profiles. (e.g. density)
- Prediction from previous step (in Kalman filter)
- Well-trained neural network

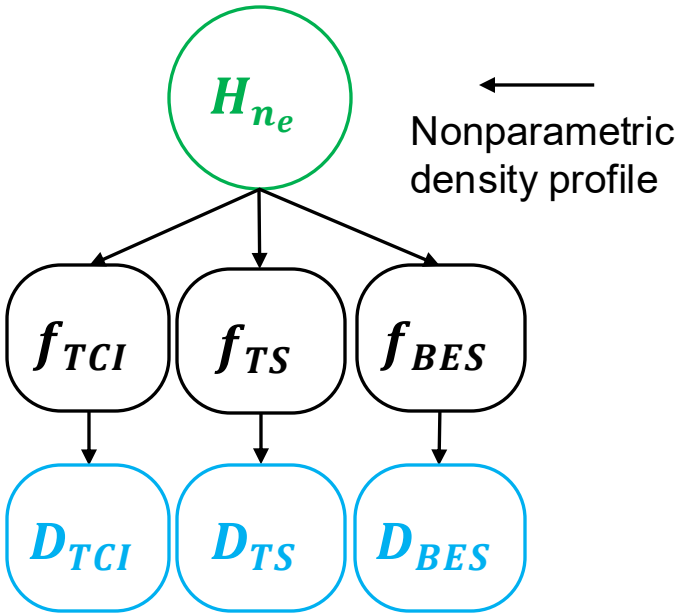

Nonparametric density profile

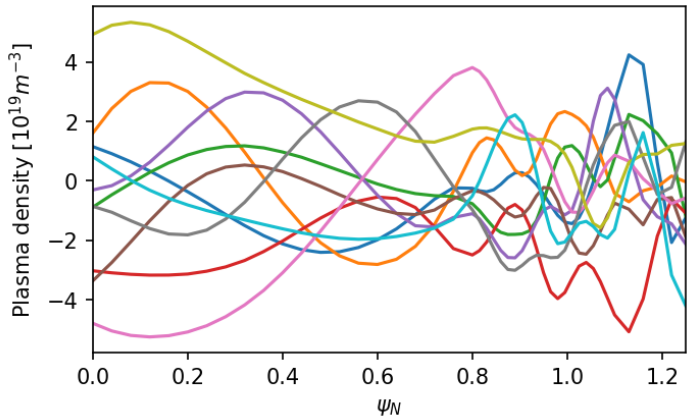

Density profile samples from Gaussian process

Add more diagnostic data and more informative prior

$$P(H|D_1, \dots, D_n, \bar{\theta}_1, \dots, \bar{\theta}_n)$$
$$\propto P(D_1|H) \dots P(D_n|H) P(H|\bar{\theta}_1) \dots P(H|\bar{\theta}_n)$$

The posterior become sharper -> leading to better estimation

- TS+TCI+BES density profile estimation
- Hall sensor + inductive coil probe for drift-free magnetic field estimation
- Nonnegativity for bolometer tomography

Data Fusion of GP prior, TS and TCI for density profile estimation

$P(\bar{n}_e|\bar{\theta})$

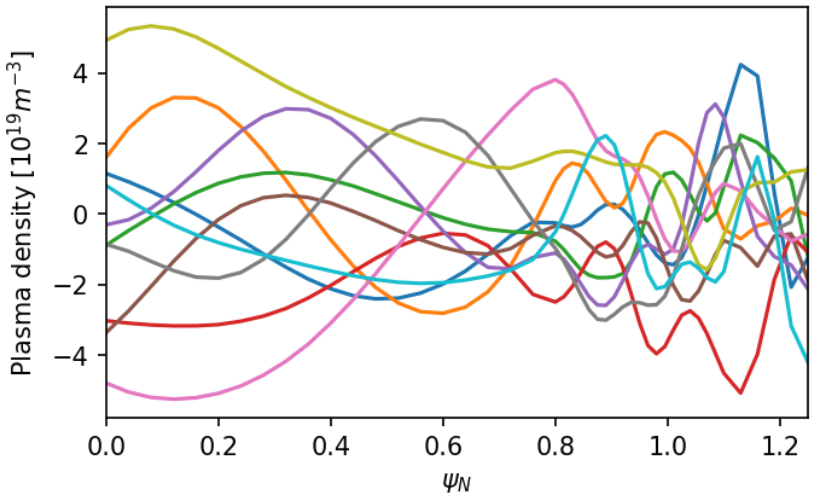

$P(\bar{n}_e|\bar{\theta})\ P(\bar{d}_{TCI}|\bar{n}_e,\bar{\theta})$

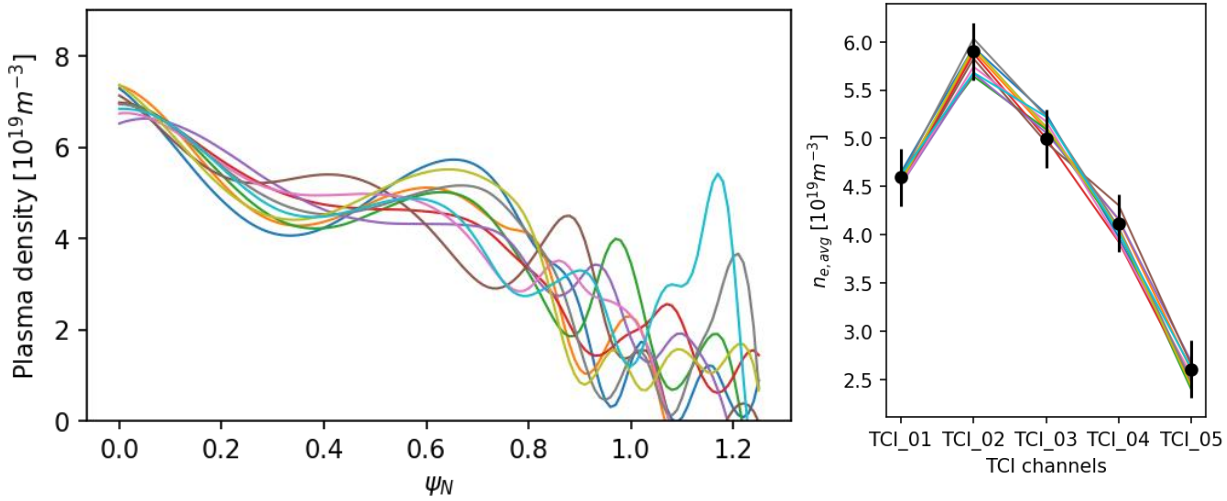

$P(\bar{n}_e|\bar{\theta})P(\bar{d}_{TS}|\bar{n}_e,\bar{\theta})$

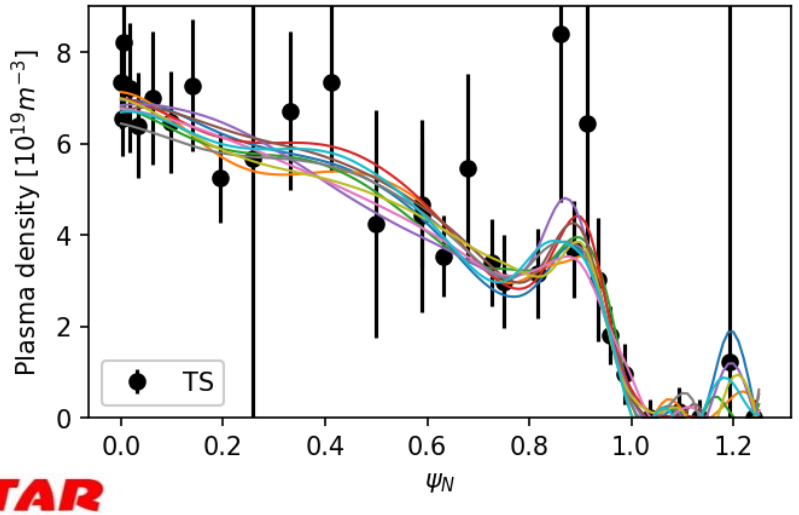

$P(\bar{n}_e|\bar{\theta})P(\bar{d}_{TS}|\bar{f},\bar{\theta})\ P(\bar{d}_{TCI}|\bar{n}_e,\bar{\theta})$

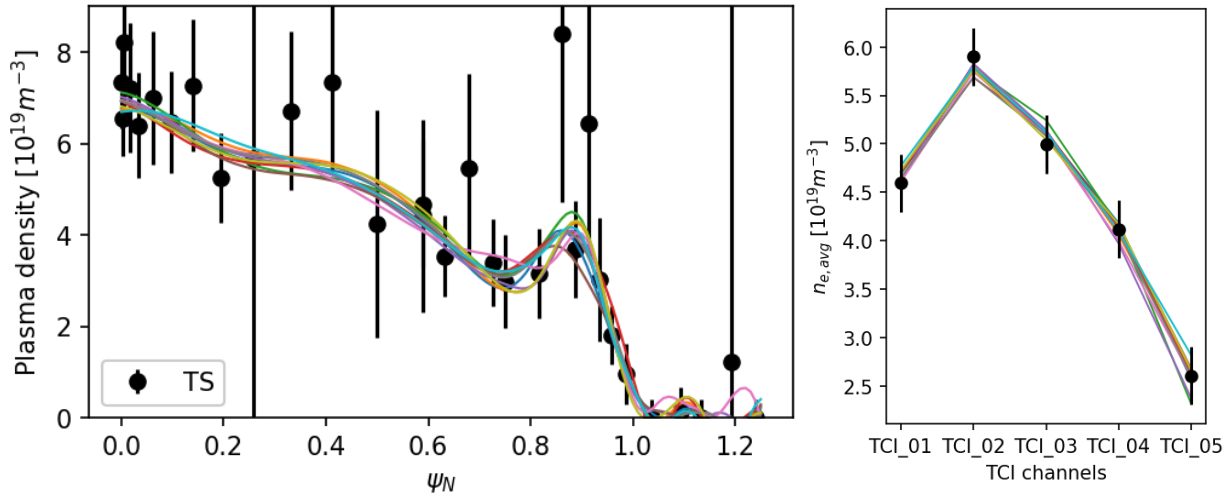

KSTAR

Edge density profile refinement by using TCI, Thomson scattering and BES

Deuterium Beam Emission Spectroscopy (BES) in KSTAR

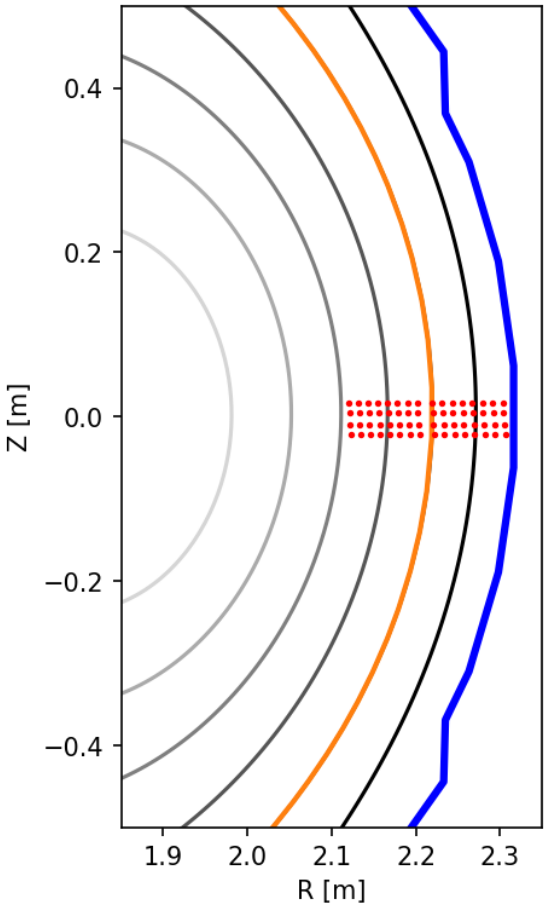

BES detecting position
on NBI1-A plane at #28030

Top view of the KSTAR BES observation geometry
[M. Lampert, RSI **86**, (2015)]

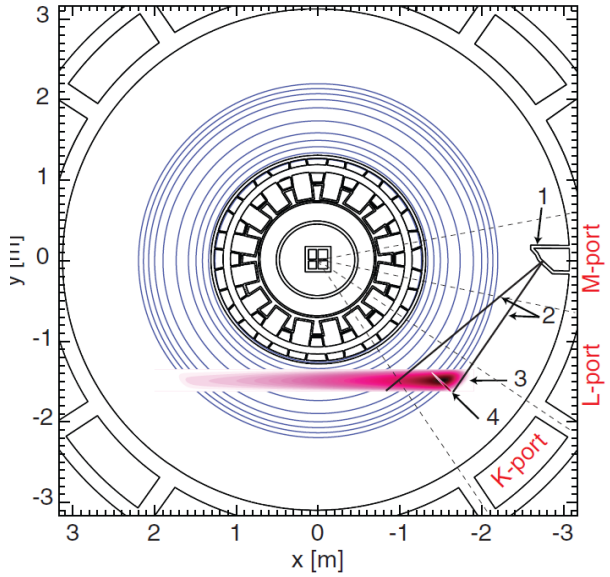

Neutral Beam injected into the plasma

↓

Deuterium atoms react with plasma particles

↓

Excitation, ionization, charge exchange,
spontaneous emission occurs

↓

Collect Doppler-shifted D_α emission (~660 nm)

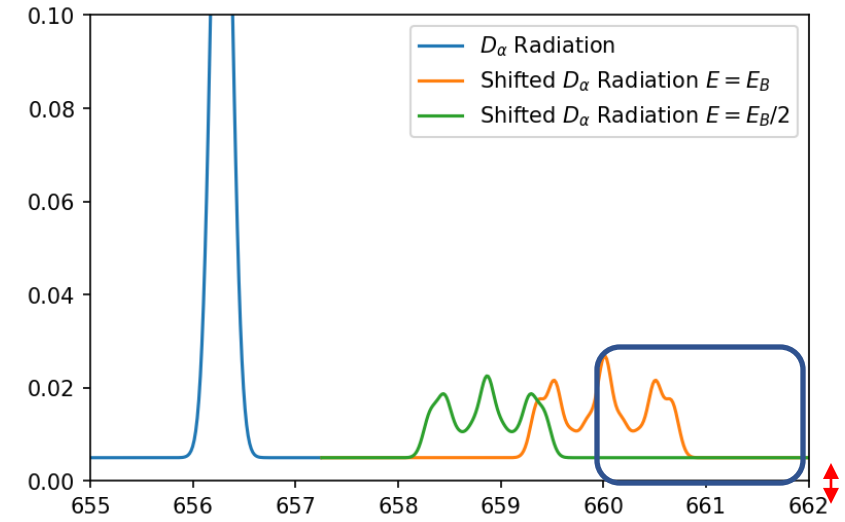

Background subtraction
+ Relative intensity calibration

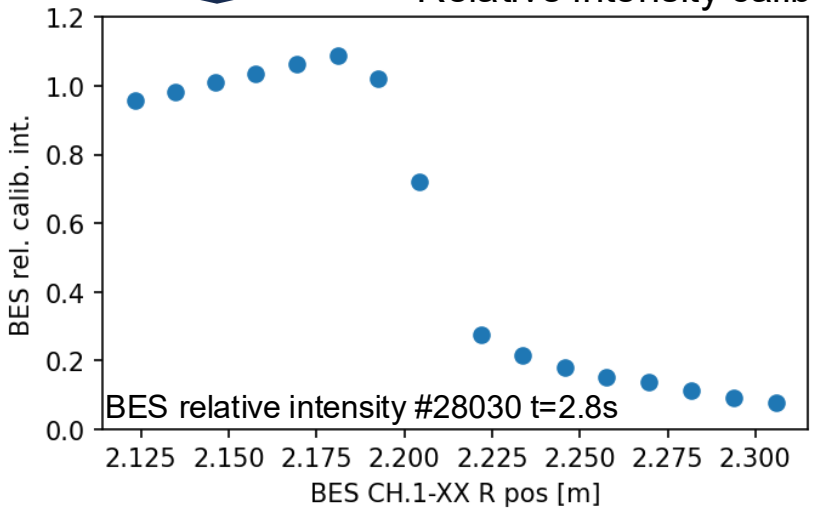

Collisional Radiative model for beam-plasma interaction

$$\frac{dn_p}{dt} = -\left[\sum_{q\neq p}\left(n_e X^e_{pq} + n_i X^i_{pq}\right) + \sum_{q<p} A_{pq}\right] n_p$$

$$+\left[\sum_{q\neq p}\left(n_e X^e_{qp} + n_i X^i_{qp}\right) + \sum_{q>p} A_{qp}\right] n_q + \left[\alpha_p + \beta_p + \gamma_{d,p}\right] n_i n_e$$

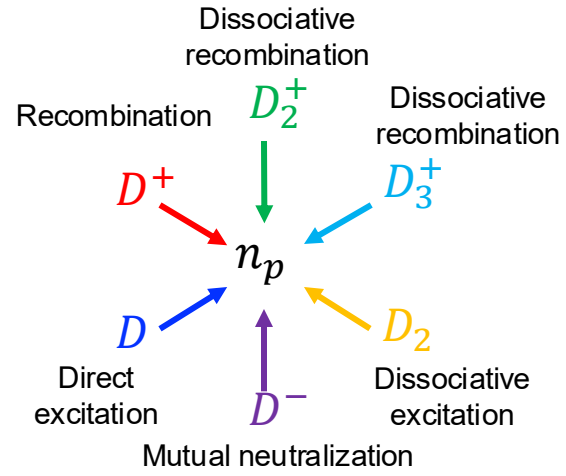

Decreasing population

Ion & electron collisional de-excitation

Spontaneous emission

Ionisation

Increasing population

Ion & electron collisional excitation

Spontaneous emission

Recombination

For BES, solve multivariable ODE,

$$\text{e.g., } \bar{\bar{X}}^e = \begin{bmatrix} -\sum_{q\neq 1} X^e_{1,q} & X^e_{2,1} & \cdots & X^e_{11,1} & X^e_{12,1} \\ X^e_{1,2} & -\sum_{q\neq 2} X^e_{2,q} & \cdots & X^e_{11,2} & X^e_{12,2} \\ \vdots & \vdots & \ddots & \vdots & \vdots \\ X^e_{1,11} & X^e_{2,11} & \cdots & -\sum_{q\neq 11} X^e_{11,q} & X^e_{12,11} \\ X^e_{1,12} & X^e_{2,12} & \cdots & X^e_{11,12} & -\sum_{q\neq 12} X^e_{12,q} \end{bmatrix}$$

$$\frac{d}{dx}\begin{bmatrix} n_1 \\ n_2 \\ \vdots \\ n_{11} \\ n_{12} \end{bmatrix} = \frac{1}{v}\frac{d}{dt}\begin{bmatrix} n_1 \\ n_2 \\ \vdots \\ n_{11} \\ n_{12} \end{bmatrix} = \left[\bar{\bar{X}}^e n_e + \bar{\bar{X}}^i n_i + \bar{\bar{A}}\right]\begin{bmatrix} n_1 \\ n_2 \\ \vdots \\ n_{11} \\ n_{12} \end{bmatrix}$$

Beam-plasma simulation by given plasma profile

TCI + Thomson scattering

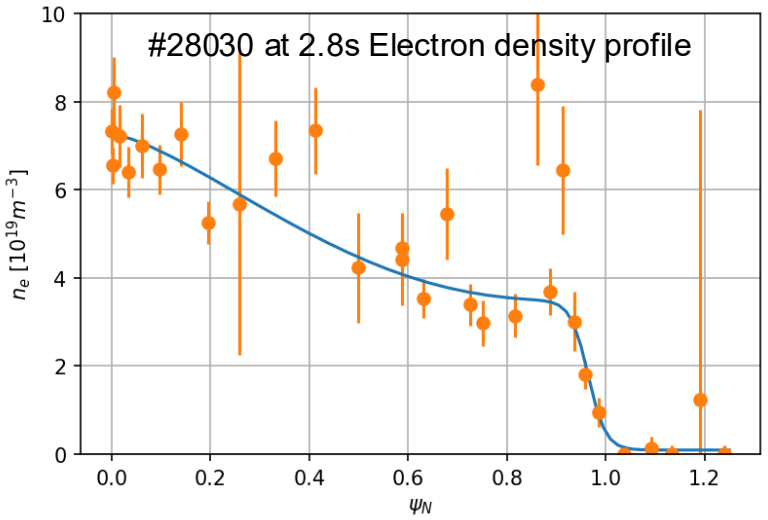

Thomson scattering

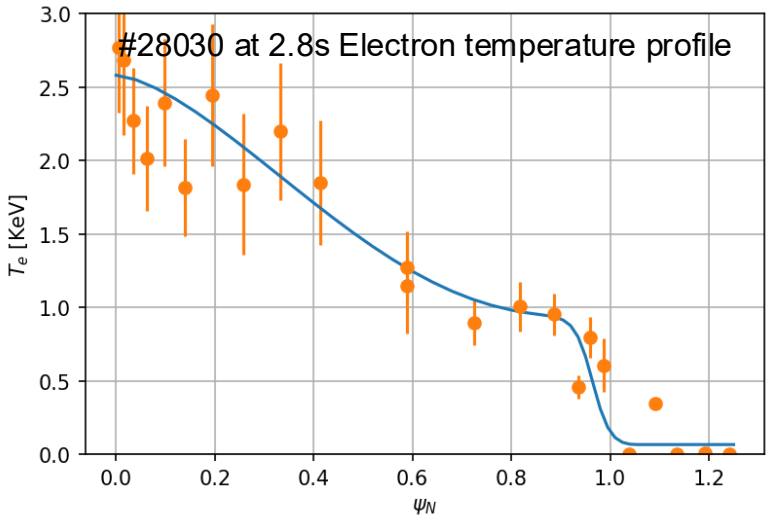

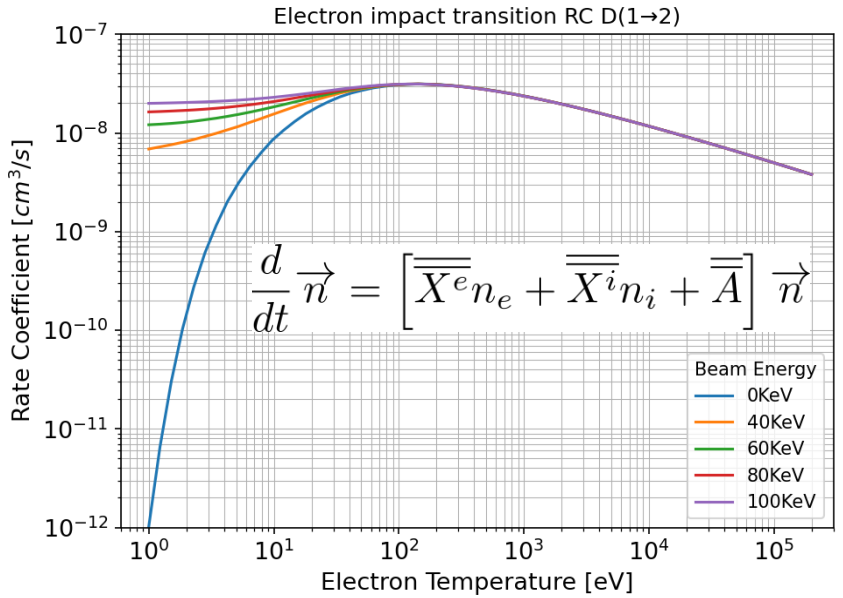

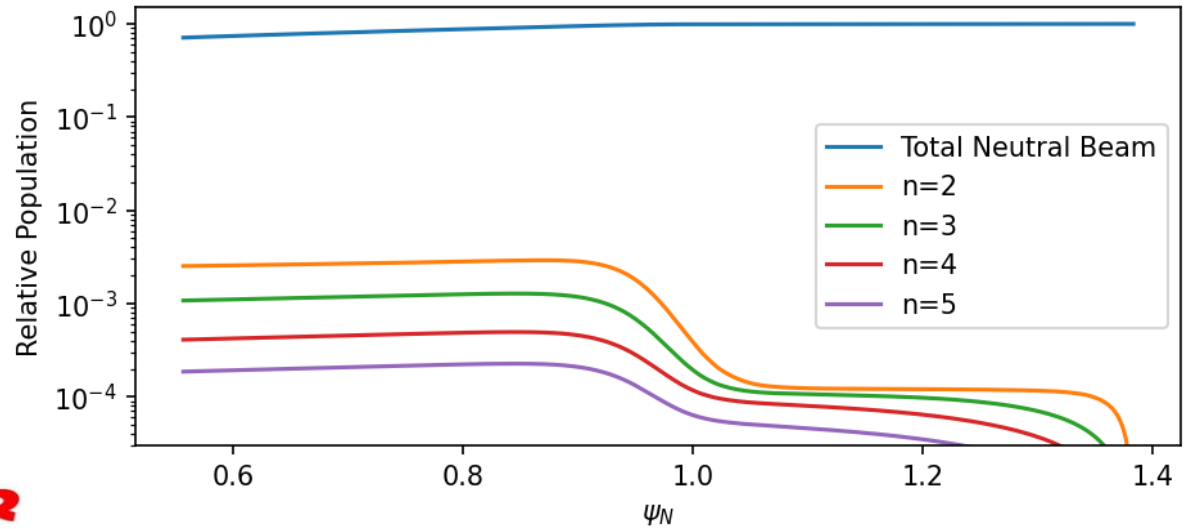

BES intensity and N=3 population profile does not match

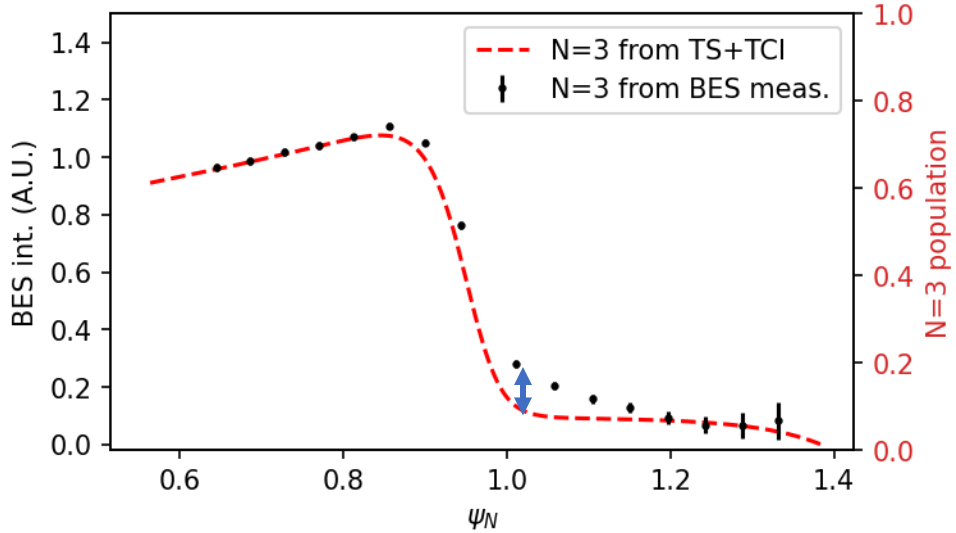

Bayesian Graphical Model for BES, TCI and TS

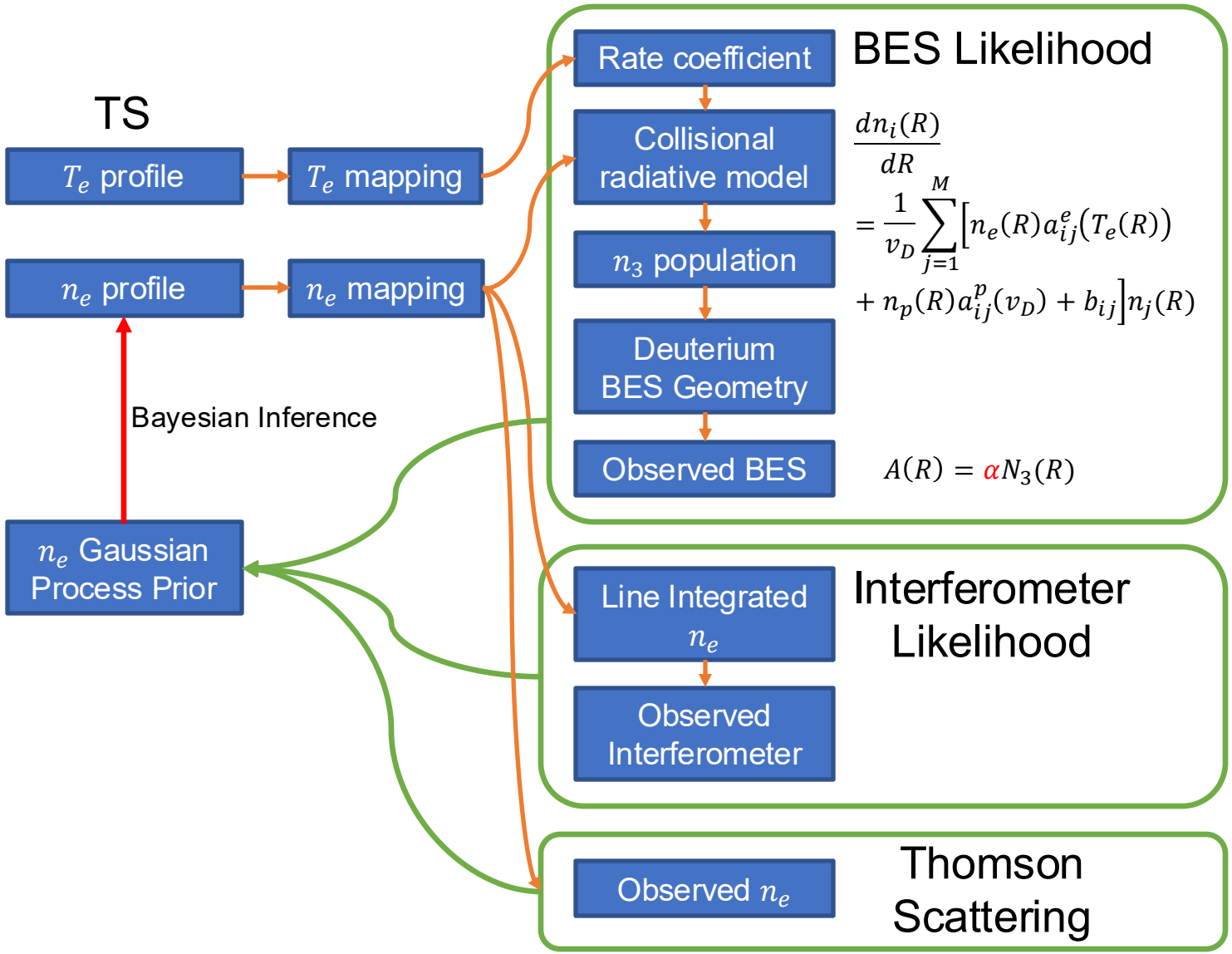

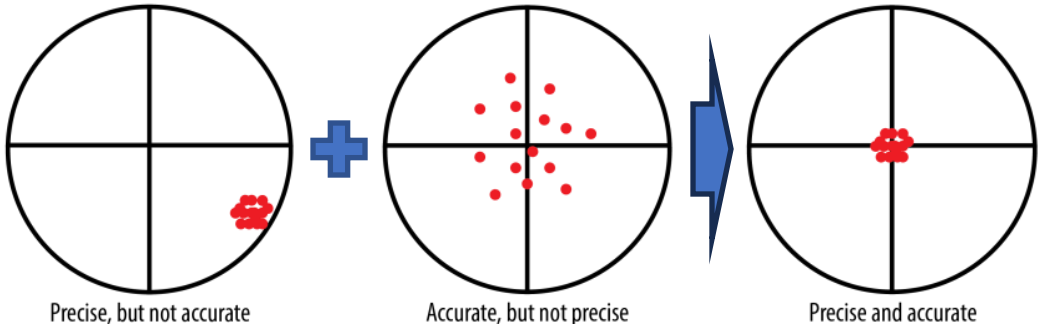

Main purpose of Hydrogen Beam Emission Spectroscopy (HBES) is edge density fluctuation measurement

- Cons: Hard to measure absolute electron density profile

Thomson scattering (TS) is essential diagnostic for electron density and temperature measurement with good accuracy

- Cons: Low precision at edge & lack of edge channel number

Interferometer have good precision

- Cons: Measure line integrated electron density

Data fusion of TS, TCI and BES for beam-plasma simulation and plasma density estimation

Bayesian inference

$$P(\bar{f}|\bar{d},\bar{\theta}) \propto P(\bar{d}|\bar{f},\bar{\theta})P(\bar{f}|\bar{\theta})$$

Data Fusion for BES, Thomson scattering and TCI

$$P(\bar{n}_e|\bar{d}_{BES},\bar{d}_{TS},\bar{d}_{TCI},\bar{\theta}) \propto P(\bar{n}_e|\bar{\theta})P(\bar{d}_{BES}|\bar{n}_e,\bar{\theta})P(\bar{d}_{TS}|\bar{n}_e,\bar{\theta})\ P(\bar{d}_{TCI}|\bar{n}_e,\bar{\theta})$$

MCMC is used to find distribution

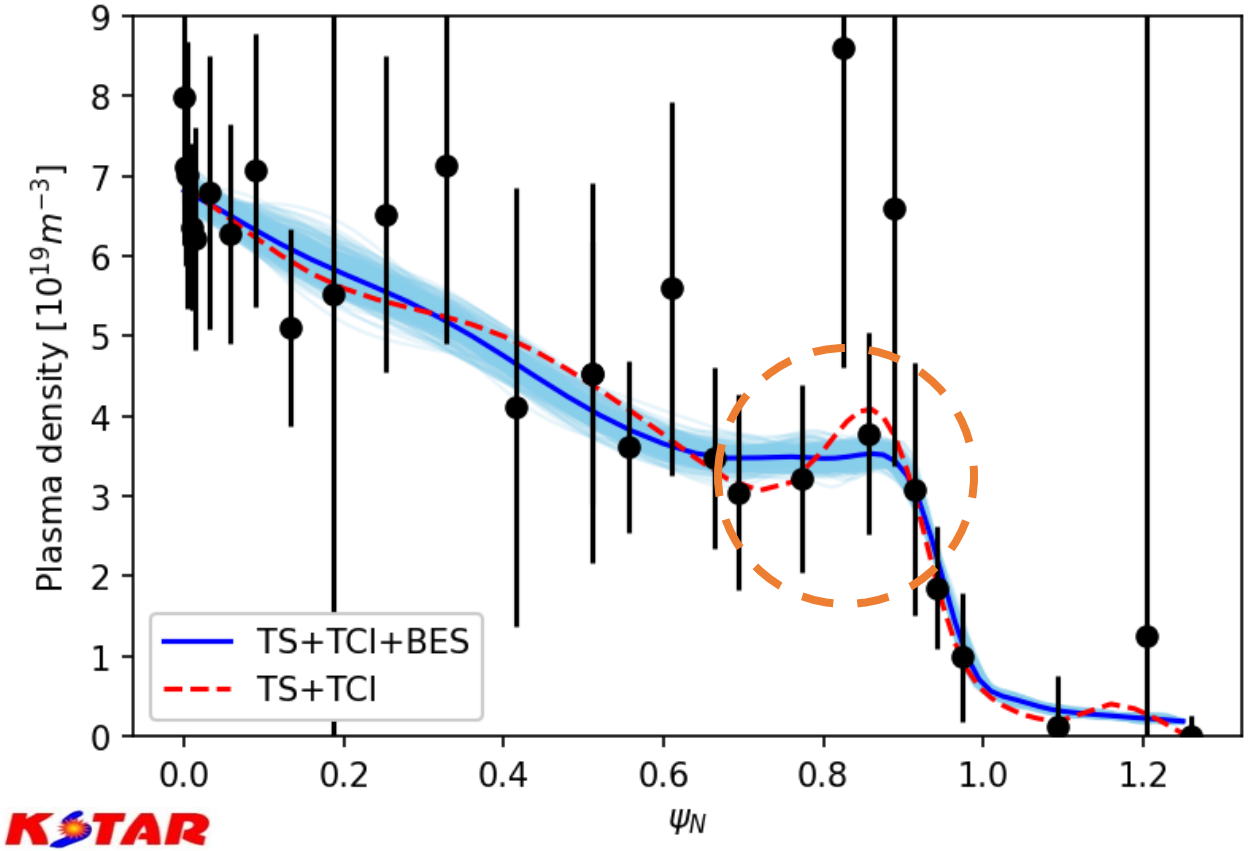

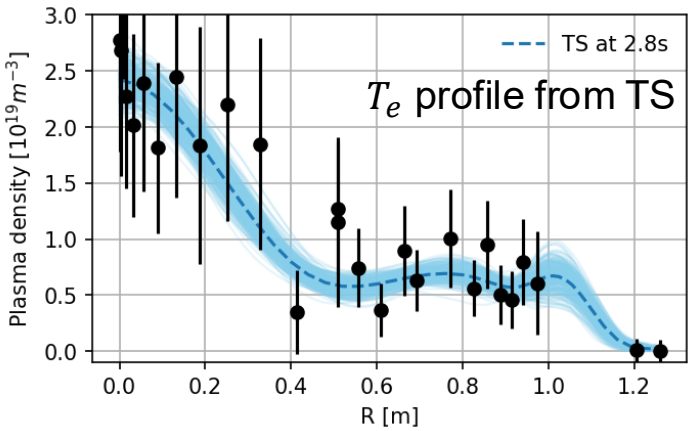

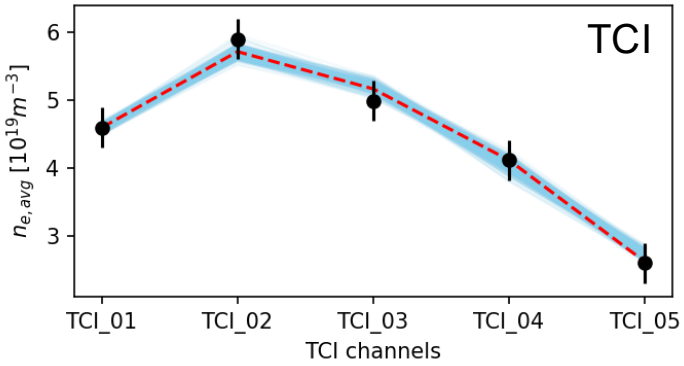

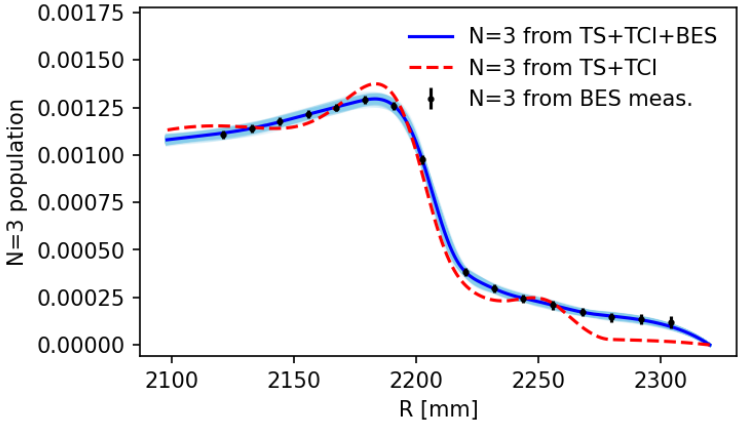

BES absolute calibration factor

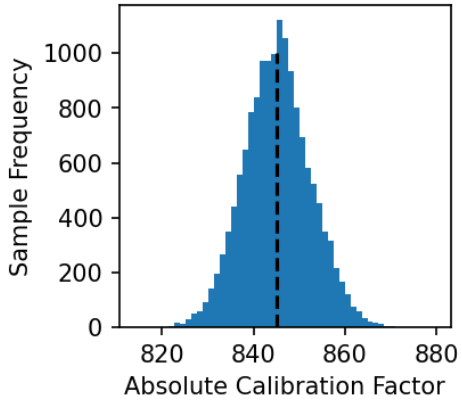

Sensor fusion of magnetic coil and Hall sensor

Sensor Fusion and Magnetic Drift Estimation in Magnetic Measurements Using Kalman Filter for Long-Duration Plasma Operations

Jaewook Kim, Jayhyun Kim, Young-chul Ghim, and J. G. Bak

KSTAR

KFE 한국핵융합에너지연구원 KOREA INSTITUTE OF FUSION ENERGY

Magnetic Coil and Hall Effect Sensor

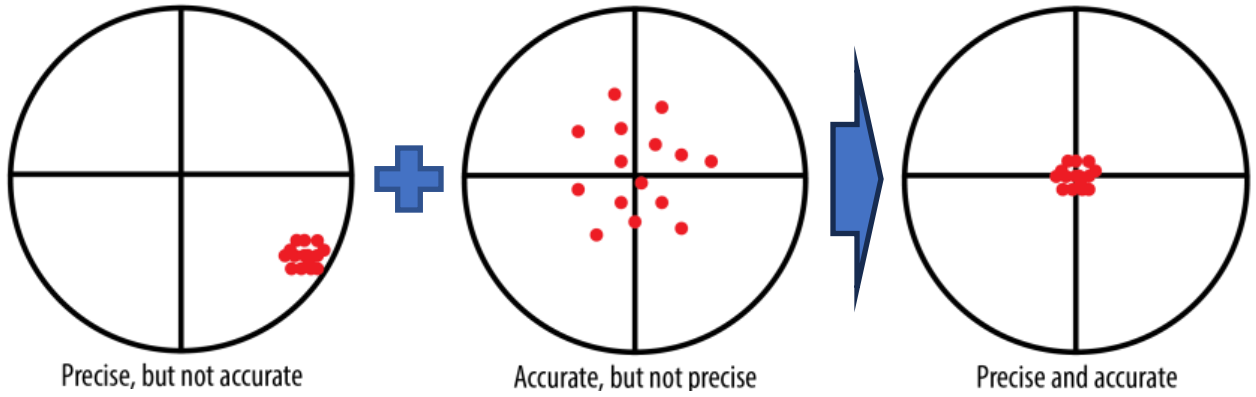

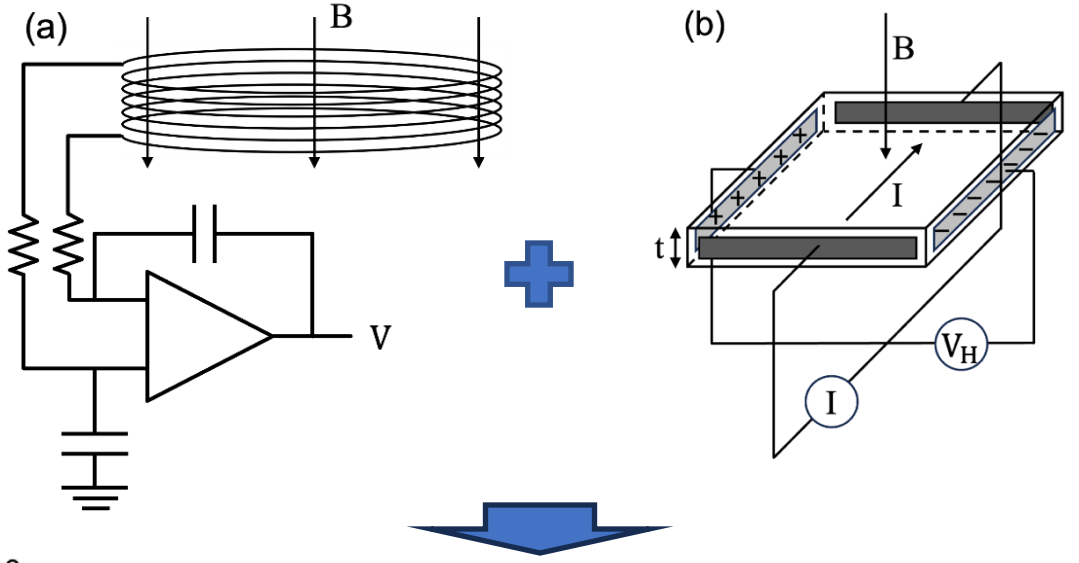

- Integrator generates "Drift" by offset
  - Radiation induced electromotive force
  - Thermo-electromotive force
  - Others…
- Hall sensor have "Low SNR"
  - Limited high-frequency response
  - Sensitivity to radiation
  - Susceptibility to electromagnetic noise
- Coil + Hall sensor : No drift and High SNR

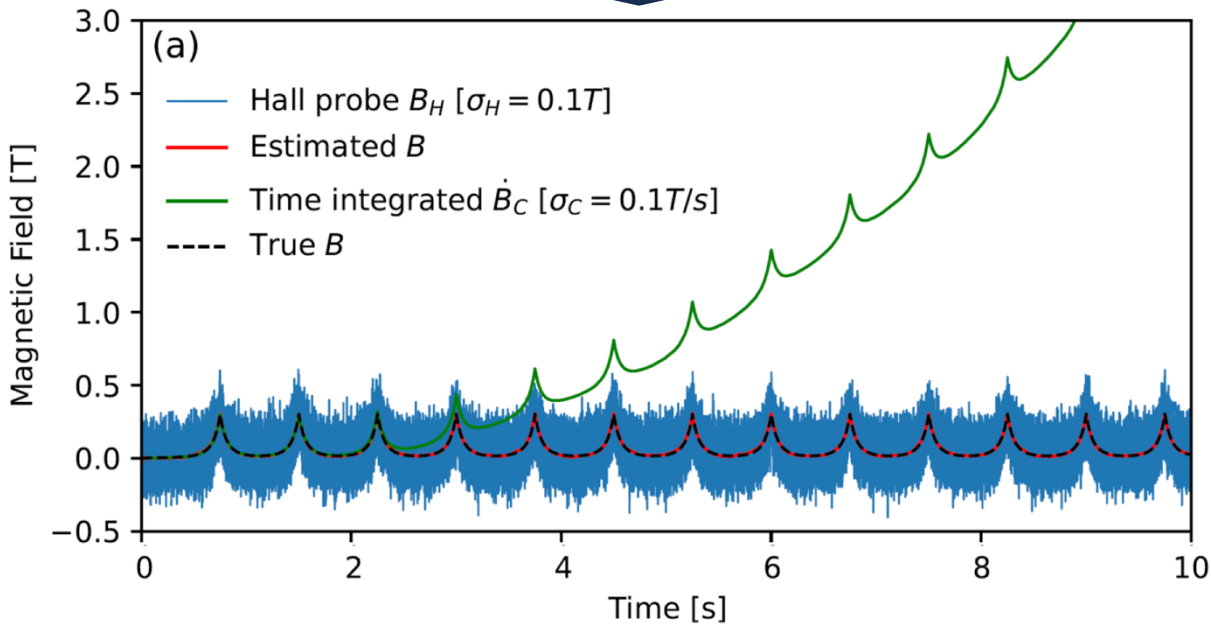

Kalman Filter (Bayes Filter with only Gaussian distribution)

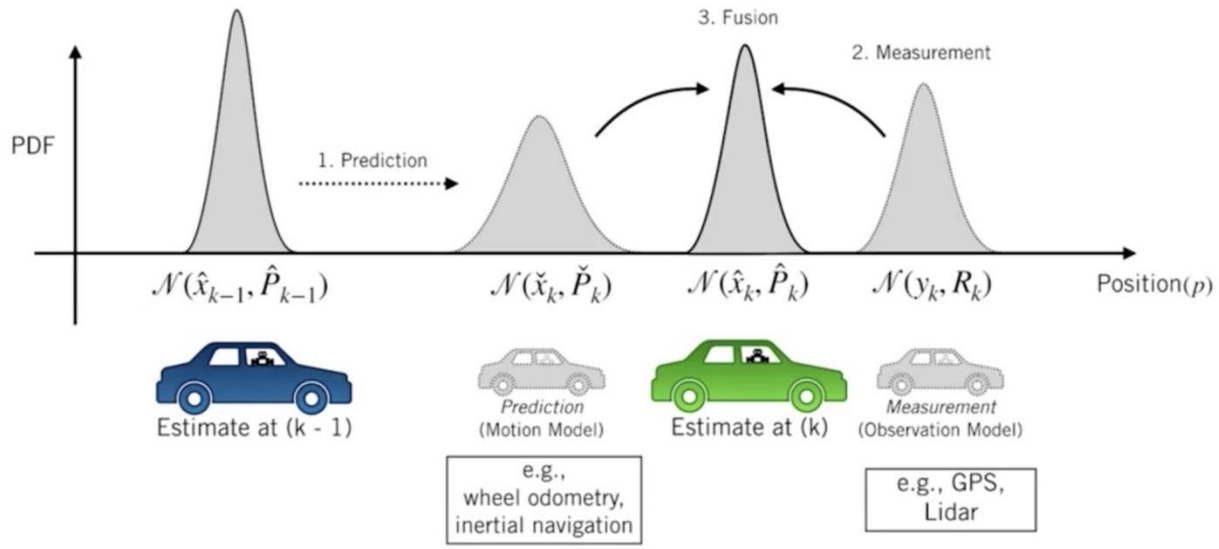

Predict: $\boldsymbol{x}_t = \boldsymbol{A}_{t-1}\boldsymbol{x}_{t-1} + \boldsymbol{B}_t\boldsymbol{u}_t + \boldsymbol{w}_t$

Correct: $\boldsymbol{z}_t = \boldsymbol{H}_t\boldsymbol{x}_t + \boldsymbol{v}_t$

$\boldsymbol{x}_0 \sim N(\boldsymbol{m}_0, \boldsymbol{P}_0),\ \boldsymbol{x}_t \sim N(\boldsymbol{m}_t, \boldsymbol{P}_t),$

$\boldsymbol{w}_t \sim N(0, \boldsymbol{Q}_t),\ v_t \sim N(0, \boldsymbol{R}_t)$

Bayes rule for bayes filter

$$P(x_t|u_1, z_1, \dots, u_t, z_t) = Z \cdot P(z_t|x_t, u_1, z_1, \dots, z_{t-1}, u_t) \cdot P(x_t|u_1, z_1, \dots, z_{t-1}, u_t)$$

Markov property of state

$$P(x_t|x_{1:t-1}, z_{t-1}, u_{t-1}) = P(x_t|x_{1:t-1})$$

$$\mathrm{Bel}(x_t) = P(x_t|u_1, z_1, \dots, u_t, z_t) = Z \cdot P(z_t|x_t) \int P(x_t|u_t, x_{t-1})\mathrm{Bel}(x_{t-1})\, dx_{t-1}$$

measurement

Prediction Step

$P(x_{t-1}|u_{0:t-1}\ z_{0:t-1}) \rightarrow P(x_t|u_{0:t}\ z_{0:t-1})$

$m_t^- = A_{t-1}\, m_{t-1}$

$P_t^- = A_{t-1}P_{t-1}A_{t-1}^T + Q_t$

Correction Step

$P(x_t|u_{0:t}\ z_{0:t-1}) \rightarrow P(x_t|u_{0:t}\ z_{0:t})$

$y_t = z_t - H_t x_t^-$

$S_t = H_t P_t^- H_t^T + R_t$

$K_t = P_t^- H_t^T S_t^{-1}$

$m_t = m_t^- + K_t y_t$

$P_t = P_t^- - K_t S_t K_t^T$

$t + 1$

State-Space model for sensor fusion (w/o drift)

- $\dot{B}_{C,t} = \dot{B}_t + \epsilon_{C,t}$ $\quad \epsilon_{c,t} \sim N(0, \sigma_c)$
- $B_{H,t} = B_t + \epsilon_H$ $\quad \epsilon_{H,t} \sim N(0, \sigma_H)$
- The state-space model :
  - $B_t = B_{t-1} + \dot{B}_{C,t} dt + \epsilon_{C,t} dt$ (or $B_t = B_{t-1} + \frac{\dot{B}_{C,t-1} + \dot{B}_{C,t}}{2} dt + \frac{\epsilon_{C,t} + \epsilon_{C,t-1}}{2} dt$)
  - $y_t = \epsilon_{H,t} = B_{H,t} - B_t$
- In this case, there is no offset in the coil data in the model
- Several papers made the hybrid magnetic sensor with this method [1,2]

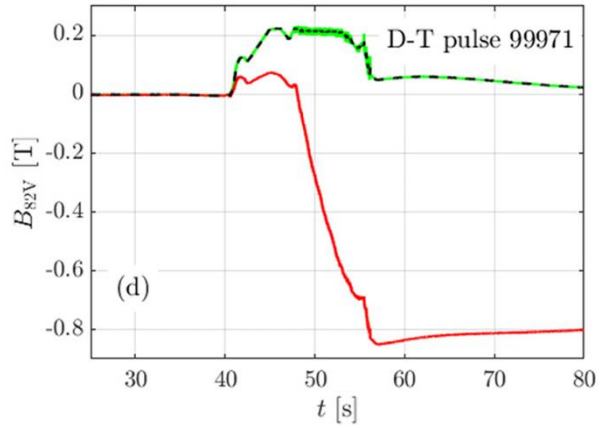

Result at [*A. Quercia et al., Nucl. Fusion 2022]

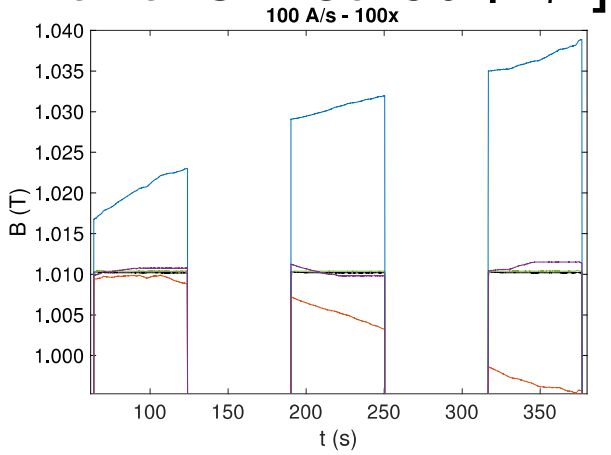

Result at [*P. Arpaia et al., Sensors 2021]

Sensor Fusion without bias estimation

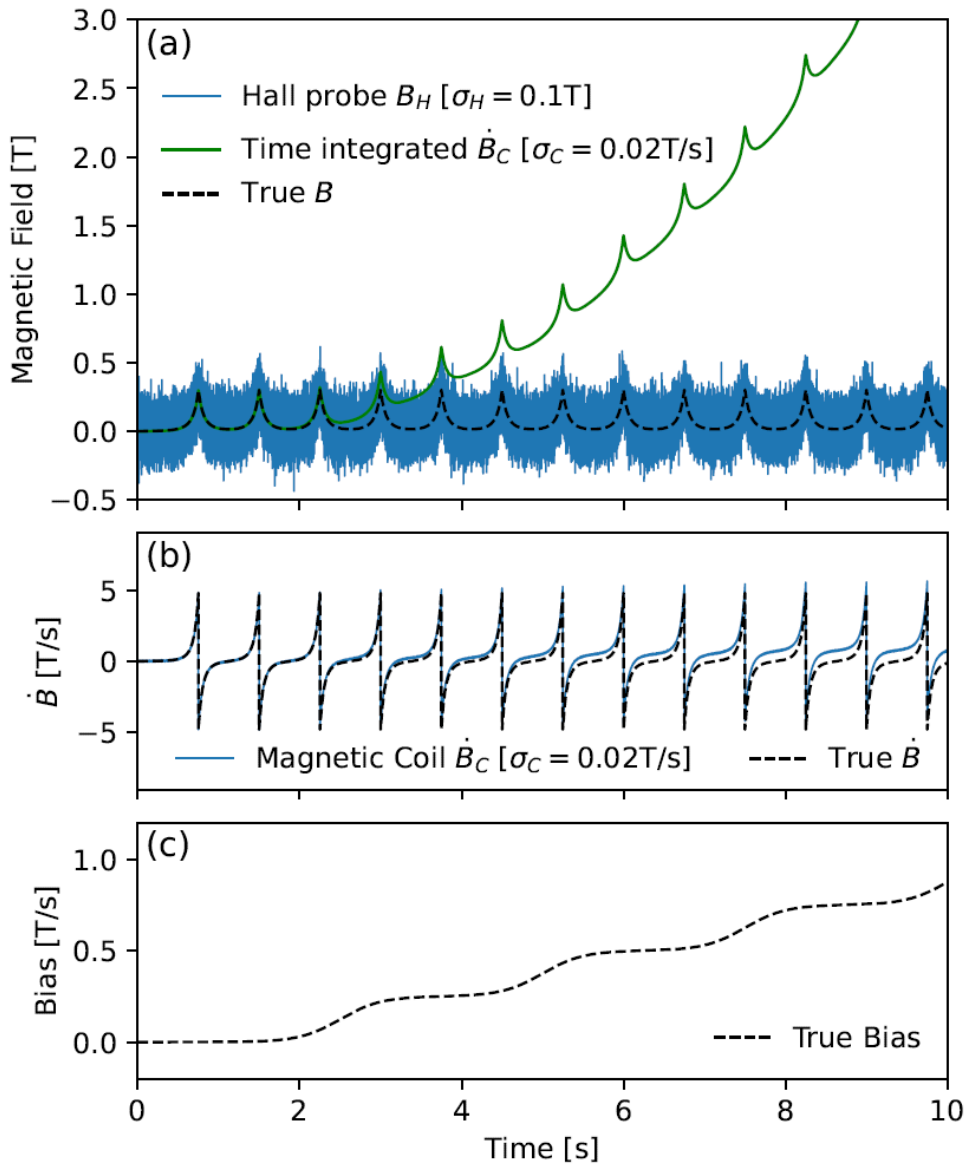

In fusion reactor…

Bias or Drift ↑
Hall sensor noise ↑

If we don't consider drift in the model…

$$V_c = NA\frac{dB}{dt} + V_{\text{bias}}$$

$$B_c(t) = B_0 + \int_0^t \frac{dB(t')}{dt'}dt' + \frac{1}{NA}\int_0^t V_{\text{bias}}(t')dt'$$

$$\dot{B}_{C,k} = \dot{B}_k + \cancel{b_k} + \epsilon_{C,k},$$
$$B_{H,k} = B_k + \epsilon_{H,k}.$$

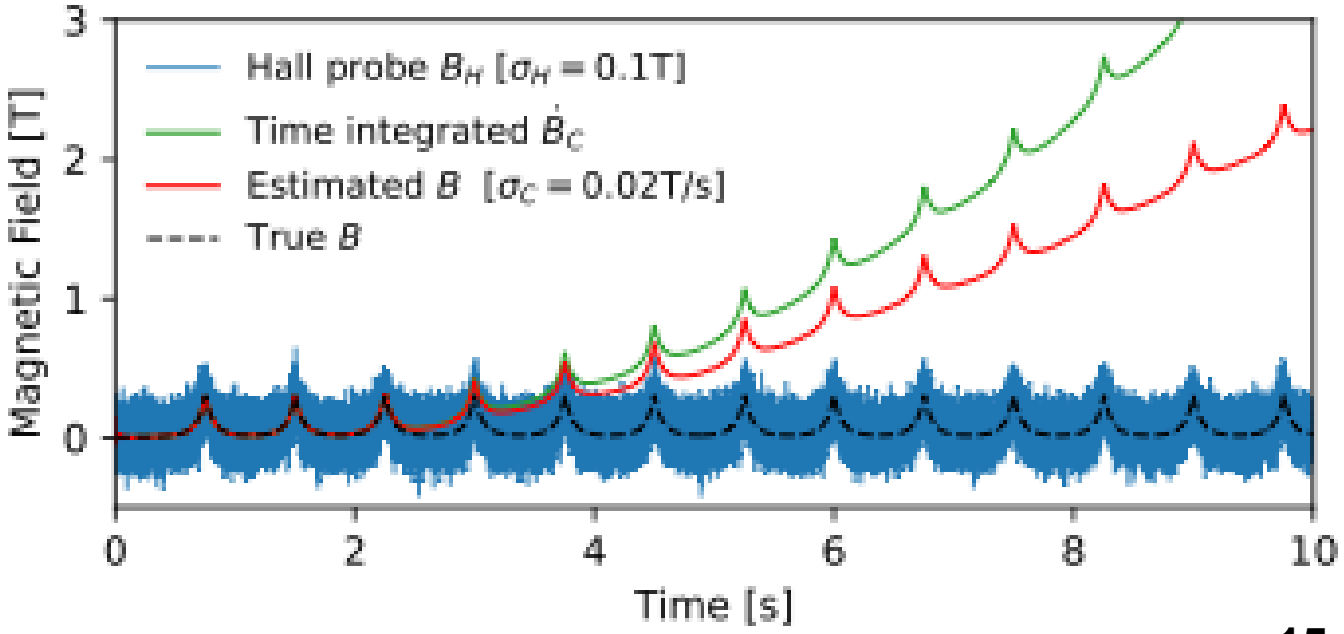

Sensor Fusion without bias estimation

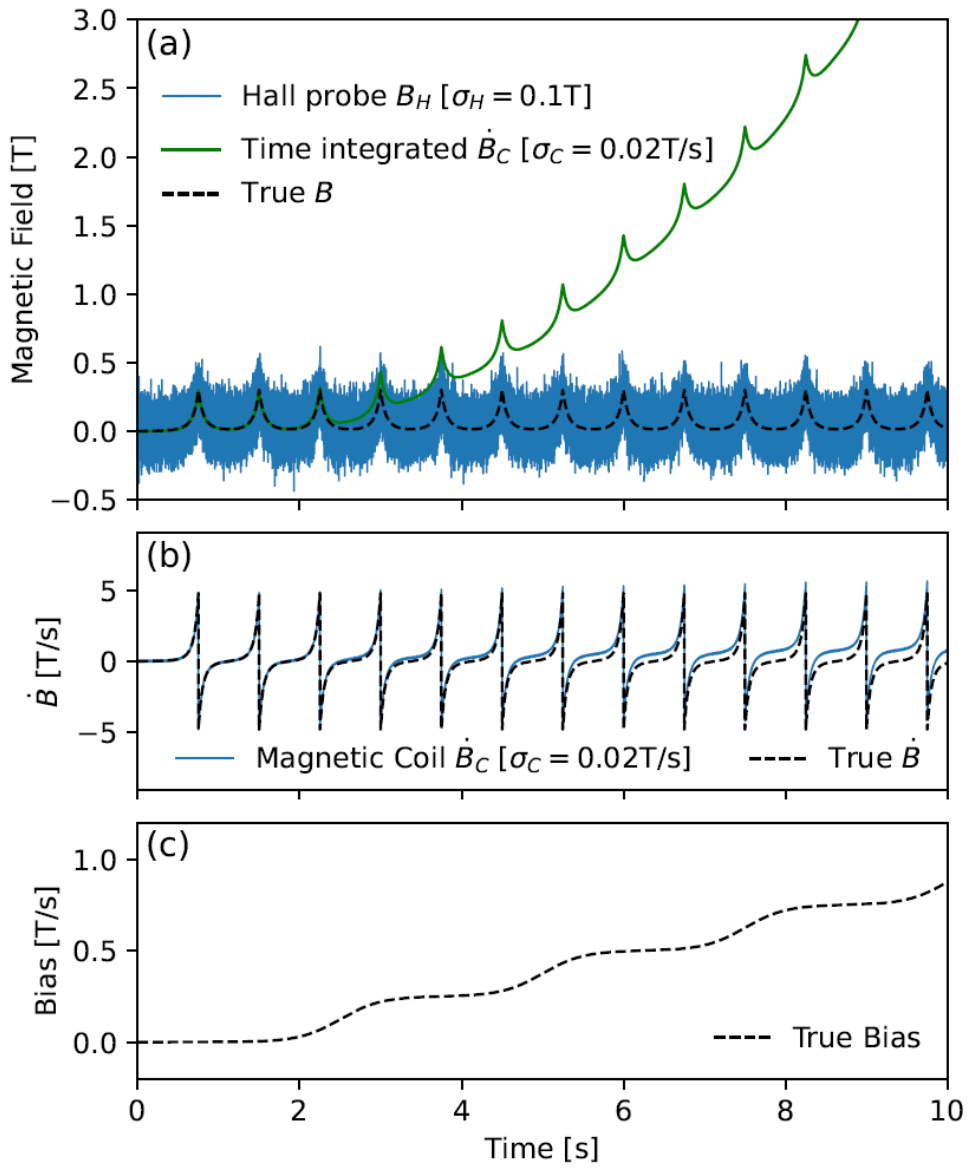

In fusion reactor…

Bias or Drift ↑
Hall sensor noise ↑

How can we model the noise?

$$V_c = NA\frac{dB}{dt} + V_{\text{bias}}$$

$$B_c(t) = B_0 + \int_0^t \frac{dB(t')}{dt'}dt' + \frac{1}{NA}\int_0^t V_{\text{bias}}(t')dt'$$

$$\dot{B}_{C,k} = \dot{B}_k + b_k + \epsilon_{C,k},$$
$$B_{H,k} = B_k + \epsilon_{H,k}.$$

b_k is a kind of Wiener process (or Brownian motion)

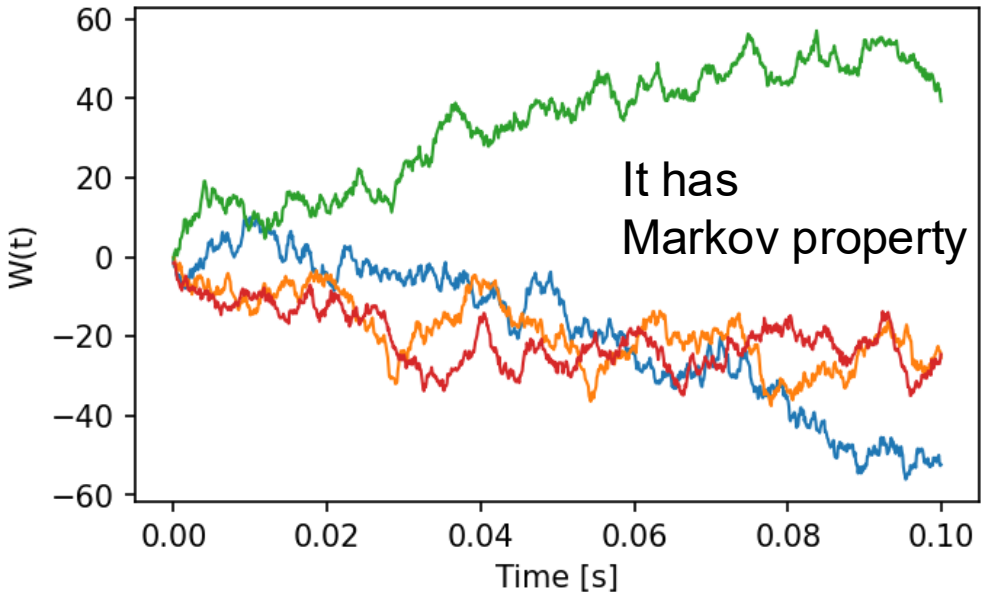

Sensor Fusion without bias estimation

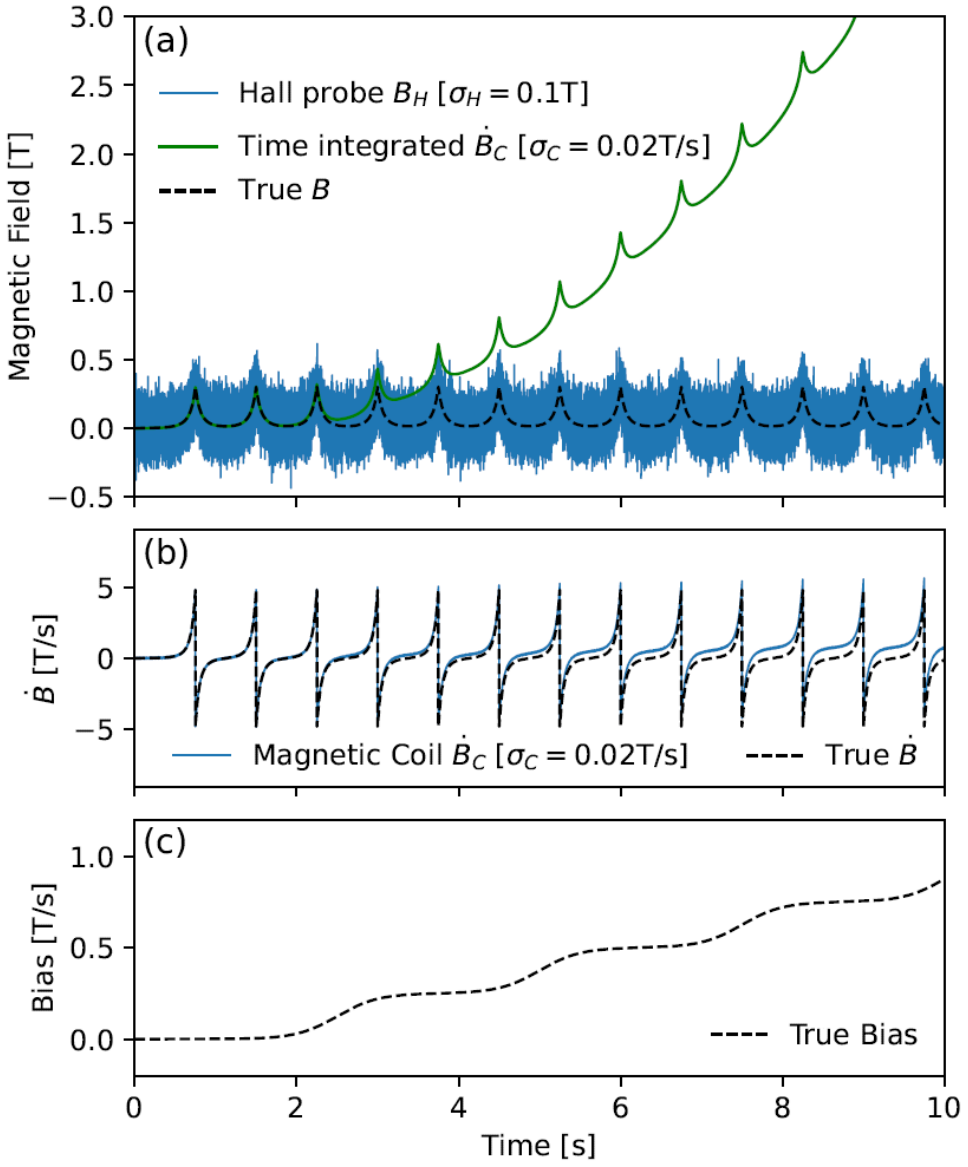

In fusion reactor…

Bias or Drift ↑
Hall sensor noise ↑

We can estimate both bias and magnetic field!

$$V_c = NA\frac{dB}{dt} + V_{\text{bias}}$$

$$B_c(t) = B_0 + \int_0^t \frac{dB(t')}{dt'}dt' + \frac{1}{NA}\int_0^t V_{\text{bias}}(t')dt'$$

$$\dot{B}_{C,k} = \dot{B}_k + b_k + \epsilon_{C,k},$$

$$B_{H,k} = B_k + \epsilon_{H,k}.$$

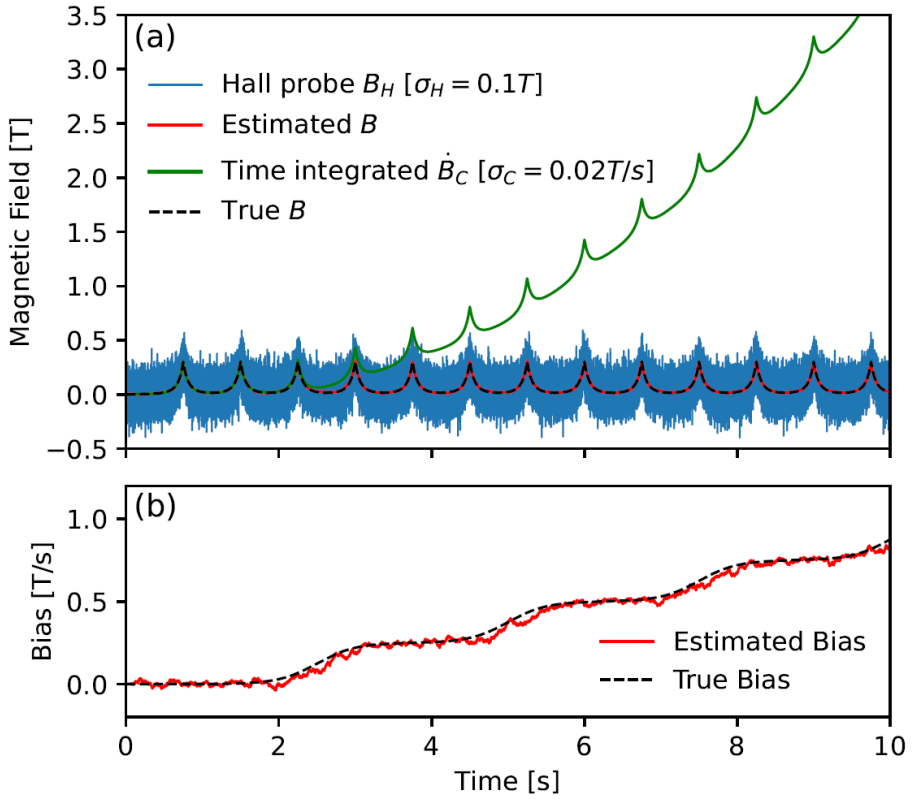

Bias step size optimization

Posterior of hypeparameters:

$$p(\theta|z_{1:k}, u_{1:k}) = \frac{p(z_{1:k}|u_{1:k}, \theta)p(\theta|u_{1:k})}{p(z_{1:k}|u_{1:k})}$$

Marginal likelihood or evidence:

$$p(\theta|z_{1:k}, u_{1:k}) \propto p(z_{1:k}|u_{1:k}, \theta)$$

$$p(z_{1:k}|u_{1:k}, \theta) = \prod_{k=0}^{T} \int p(z_k|x_k, u_{1:k}, \theta) \cdot p(x_k|z_{0:k-1}, u_{1:k}, \theta) dx_k$$

$$l_k = l_{k-1} - \frac{1}{2}\left(y_k^T S_k^{-1} y_k + \log|S_k| + d_y \log 2\pi\right)$$

Bayesian Occam's razor:
Simplest model is the best until it explain the data

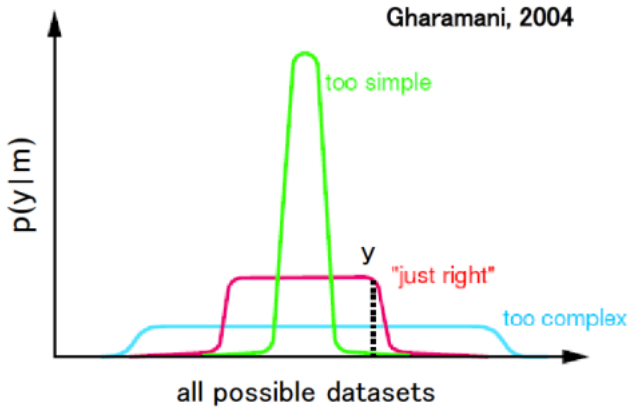

Log evidence as function of step size

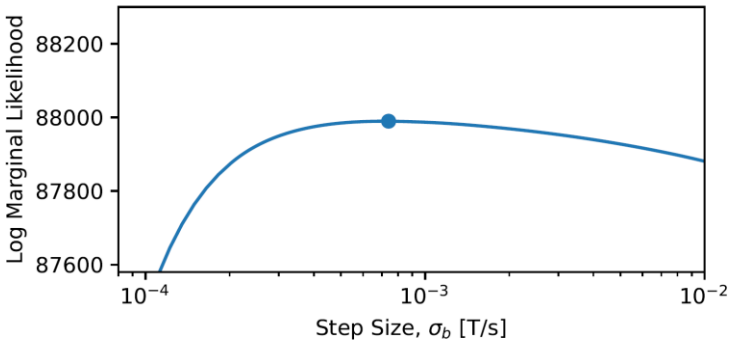

Bias estimation with optimal step size

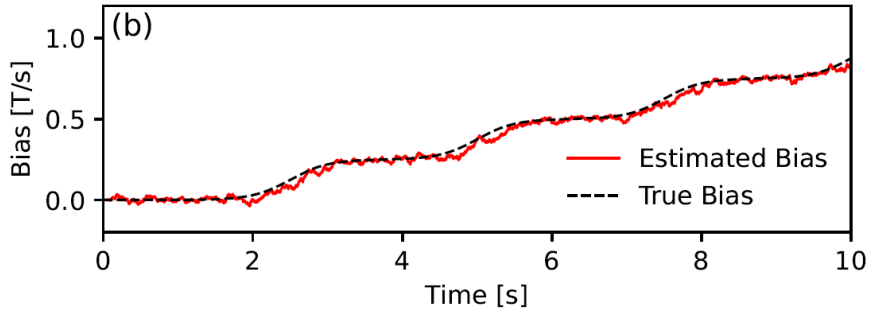

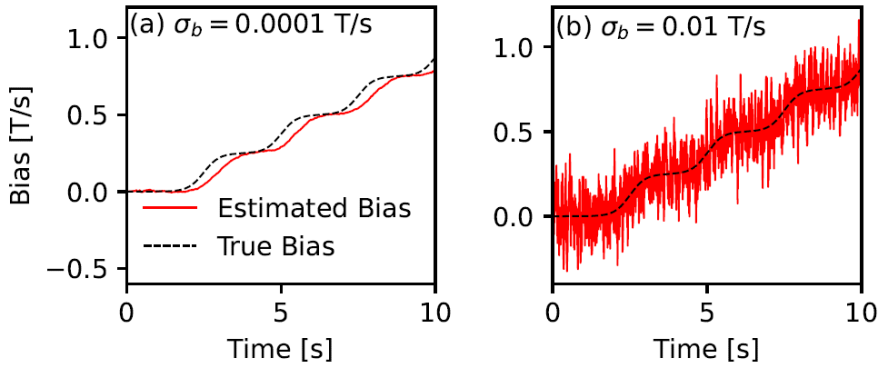

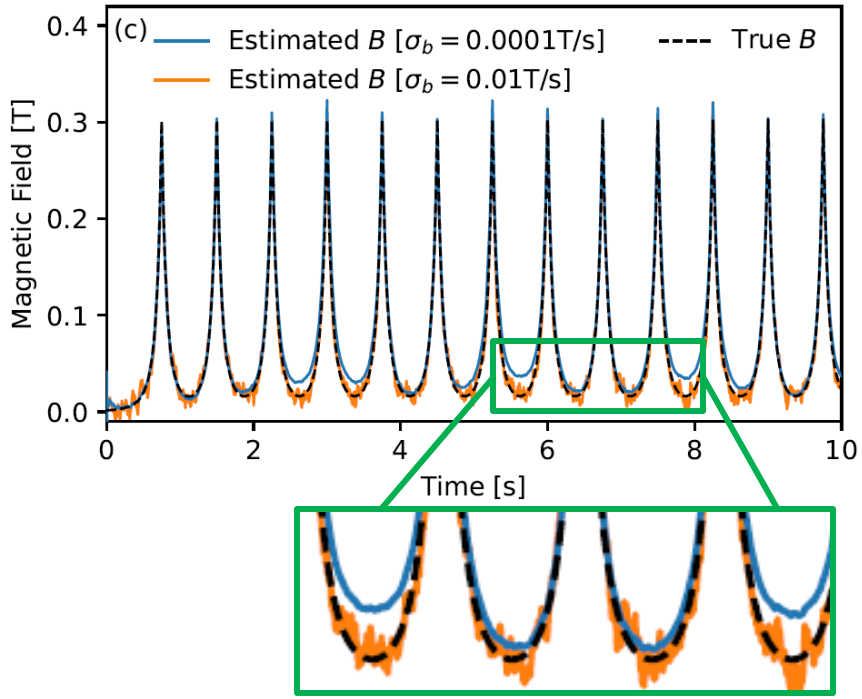

Radiation Tomography for disruption study

-Denoising quasi-coherent noise
-Gaussian process tomography with nonnegative prior

Tomography reconstruction for disruption study in KSTAR is challenging problem

- Shattered Pellets are injected at KSTAR O-port and G-port
- Poloidal Filtered AXUV arrays are installed at D-port and O-port
- Each AXUV array system is pinhole array with 20 lines of sight
- Superconductor tokamak has lack of view ports
  - PFAA systems have bad and poor line of sight arrangement

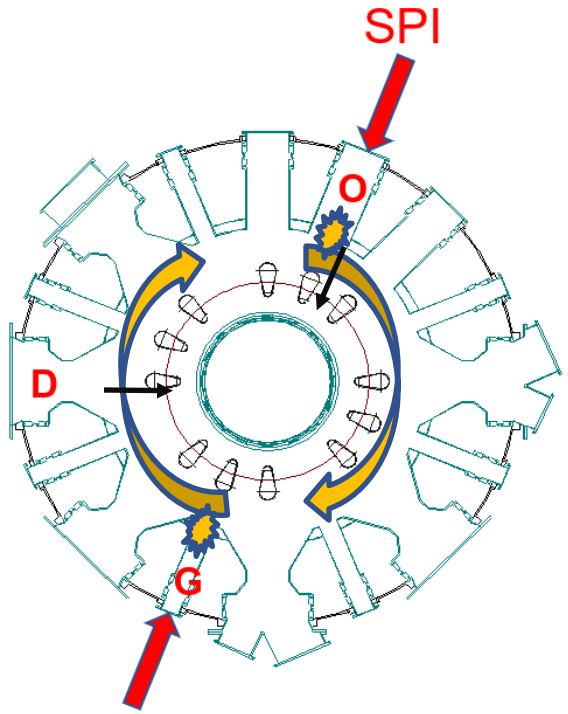

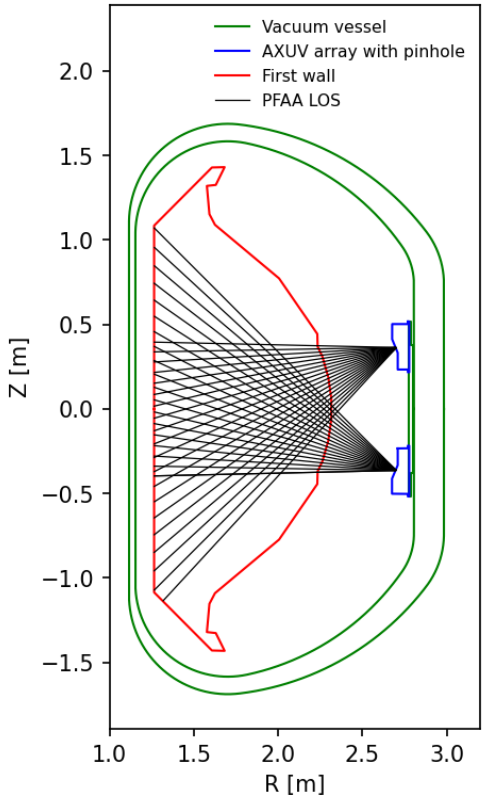

Fast visible camera data indicate plasma radiation have strong asymmetry along poloidally and toroidally during pellet induced disruption

Denoising quasi-coherent noise

Gaussian process-based quasi-coherent noise suppression in magnetic confinement devices with superconductors
J. Kim, J. Kim, Y.-C. Ghim, and J. Jang, NF **63**, 106017 (2023)

KSTAR

KFE 한국핵융합에너지연구원 KOREA INSTITUTE OF FUSION ENERGY

Large noise due to IVCC

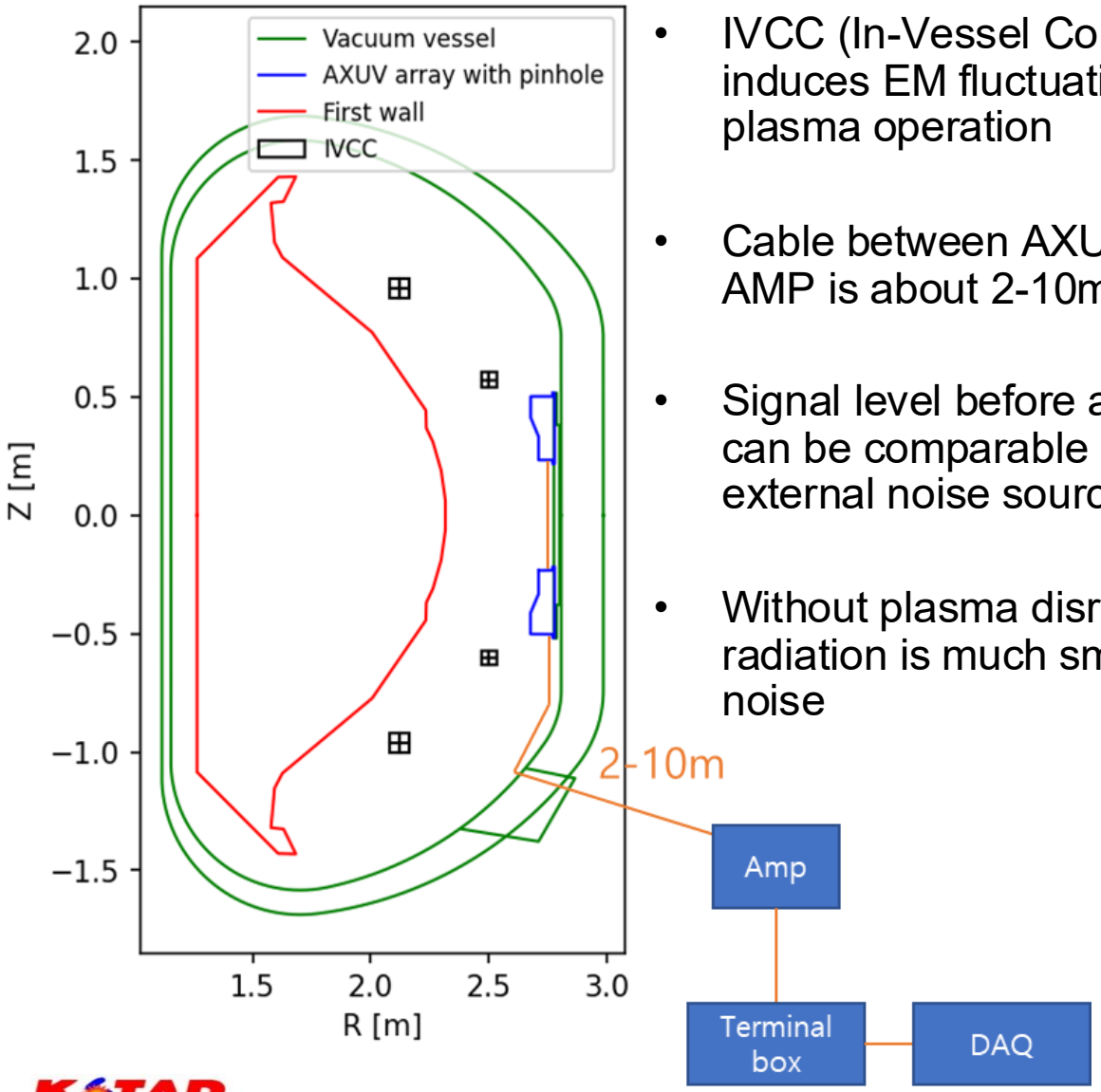

- IVCC (In-Vessel Control Coil) induces EM fluctuation during plasma operation
- Cable between AXUV array and AMP is about 2-10m
- Signal level before amplification can be comparable to the external noise source
- Without plasma disruption, radiation is much smaller than noise

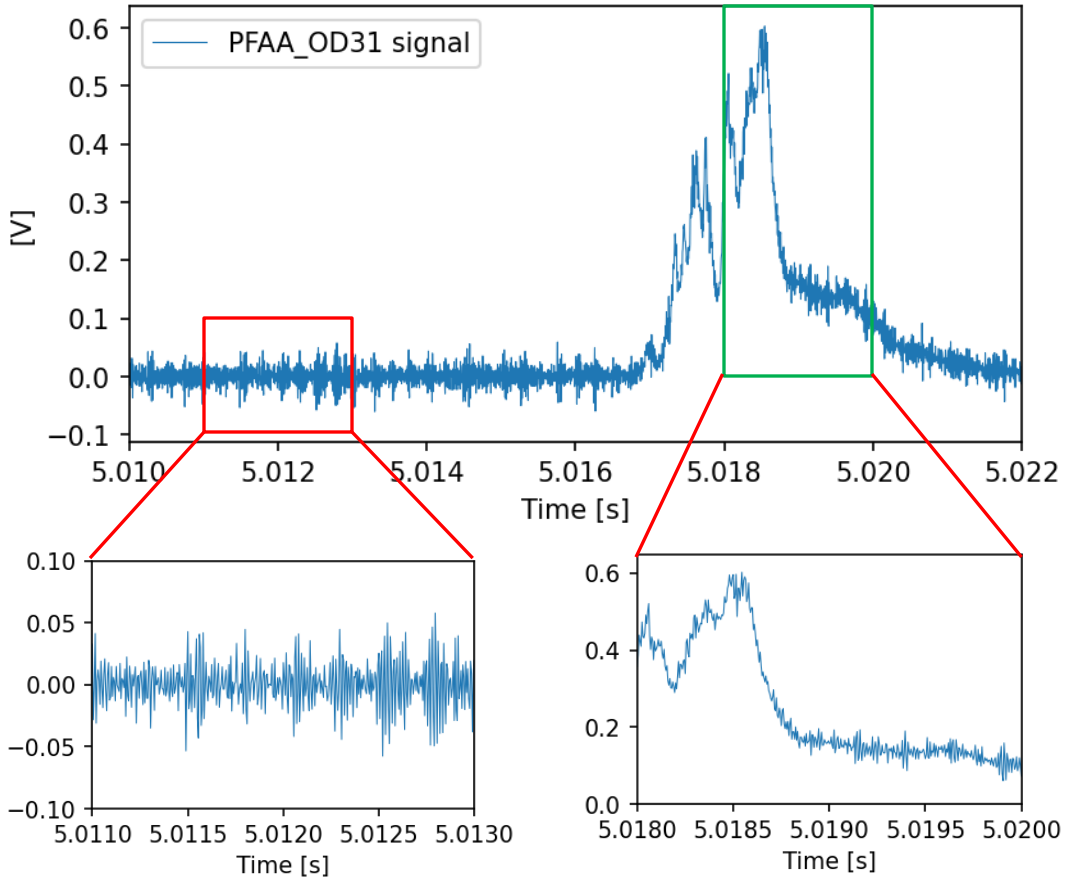

$\vec{y}(t) \simeq \vec{\epsilon}(t)$
If radiation is very small

$\vec{y}(t) = \vec{f}(t) + \vec{\epsilon}(t)$
When there is radiation due to disruption

Gaussian process regression for signal reconstruction

- The signal with noise: $\bar{y}(X) = \bar{f}(X) + \bar{\epsilon}(X)$, where $\epsilon \sim N(0, \bar{\bar{\Sigma}}_\epsilon(X,X))$
- The joint probability of given data $\bar{y}$ and $\bar{f}(X)$ [*]:

$$\begin{bmatrix} \bar{y} \\ \bar{f}(X_*) \end{bmatrix} \sim N\left(0, \begin{bmatrix} \bar{\bar{K}}(X,X) + \bar{\bar{\Sigma}}_\epsilon(X,X) & \bar{\bar{K}}(X,X_*) \\ \bar{\bar{K}}(X_*,X) & \bar{\bar{K}}(X_*,X_*) \end{bmatrix}\right)$$

- The conditional distribution of $\bar{f}(X)$ with given $\bar{y}$ will be

$$\bar{f}(X)|X_*, X, \bar{y}, \epsilon \sim \mathcal{N}\left(\bar{\bar{K}}(X,X)\left[\bar{\bar{K}}(X,X) + \bar{\bar{\Sigma}}_\epsilon(X,X)\right]^{-1}\bar{y},\right.$$
$$\left.\bar{\bar{K}}(X,X) - \bar{\bar{K}}(X,X)\left[\bar{\bar{K}}(X,X) + \bar{\bar{\Sigma}}_\epsilon(X,X)\right]^{-1}\bar{\bar{K}}(X,X)\right)$$

  - In our case, the noise is not Gaussian white noise
    - It has quasi-periodic or coherent properties
  - We predict for sampled position : $X_* \to X$
    - $\bar{\epsilon}(X) \sim N(0, \bar{\bar{\Sigma}}_\epsilon(X,X))$
    - Auto-correlation matrix :
      Toeplitz matrix of auto-correlation function
    - $\Sigma_{\epsilon,ij} = \Sigma_{\epsilon,ij} = a_{i-j}$

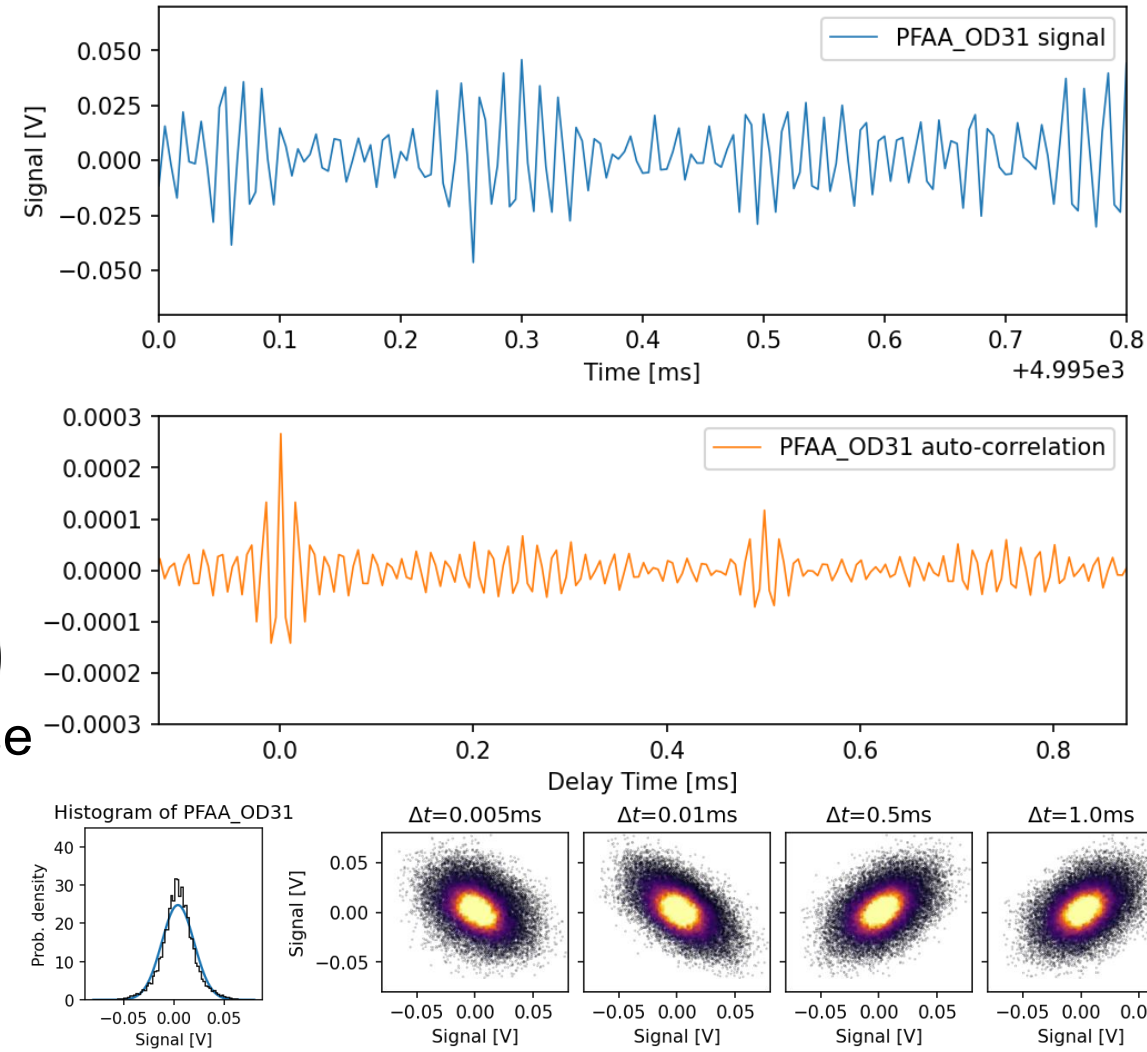

[*] David Duvenaud, *et al.*, arXiv:1112.4394 (2011)

Gaussian process regression for signal reconstruction

- Evidence maximization is used to get hyperparameter $\theta = (\sigma_f, l)$
- Model evidence : $p(y|m) = \int p(y|\theta, m)p(\theta|m)d\theta$

$$\underset{\sigma_f, l}{\operatorname{argmax}} \log p(y|\sigma_f, l, X) = \underset{\sigma_f, l}{\operatorname{argmax}} \left(-\frac{1}{2}(y-\mu)^T (K(\sigma_f, l, X) - \Sigma_\epsilon(X,X))^{-1}(y-\mu) \right.$$
$$\left. -\frac{1}{2}\log|K(\sigma_f, l, X, X) + \Sigma_\epsilon(X,X)| - \frac{n}{2}\log 2\pi \right)$$

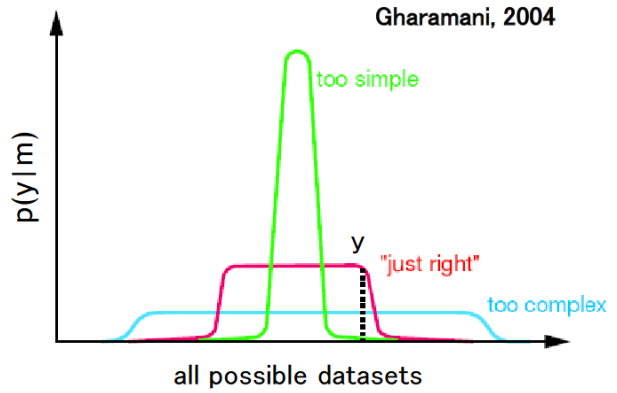

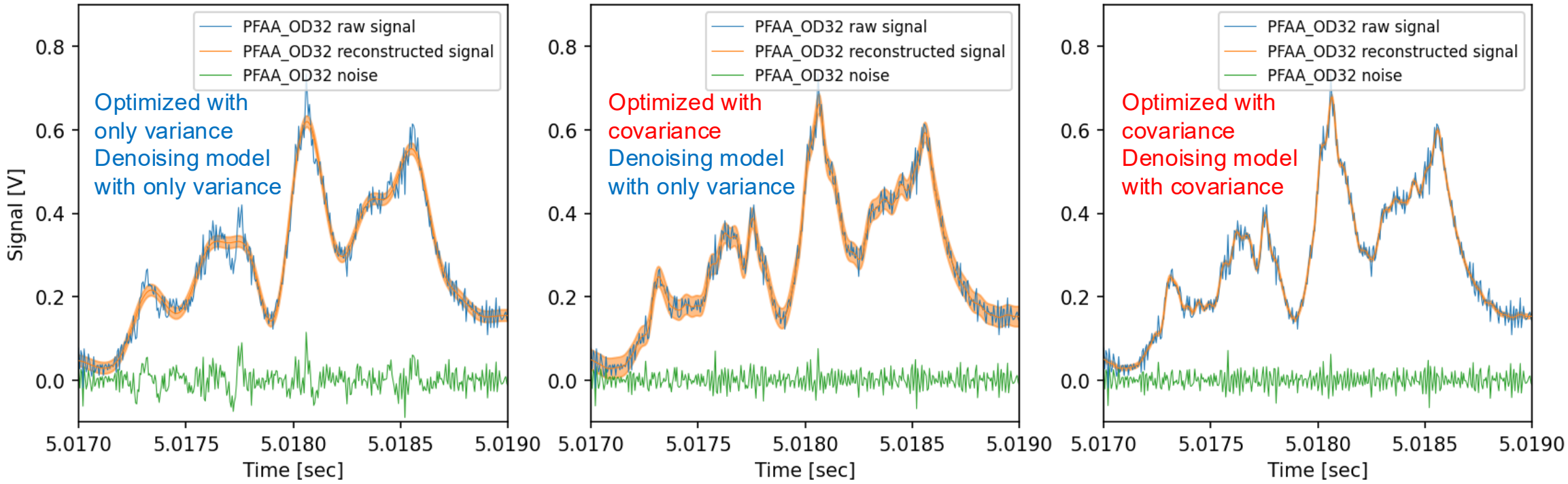

Gaussian process tomography with nonnegative prior

Tomography reconstruction is ill-posed problem

Tomography : Reconstruction of local emissivity from measured data

Pixel based tomography shares the equation:

$$\bar{d} = \bar{\bar{W}} \cdot \bar{f} + \bar{\epsilon}$$

$\bar{d}$: Line integrated signals, measured data, m vector

$\bar{\bar{W}}$: Contribution factor of local emissivity for each sensor
$m \times n$ matrix, m is # of LOS, n is # of pixel

$\bar{f}$: Local emissivity, n vector

$\bar{\epsilon}$: Uncertainty of measured data, m vector

Regularization term is needed when least square estimation has infinite solutions (e.g. $m < n$)

For KSTAR PFAA:

- Gaussian Process Tomography (GPT)
  - ✓ Tomography model + Gaussian process
  - ✓ Gaussian process is used for regularization

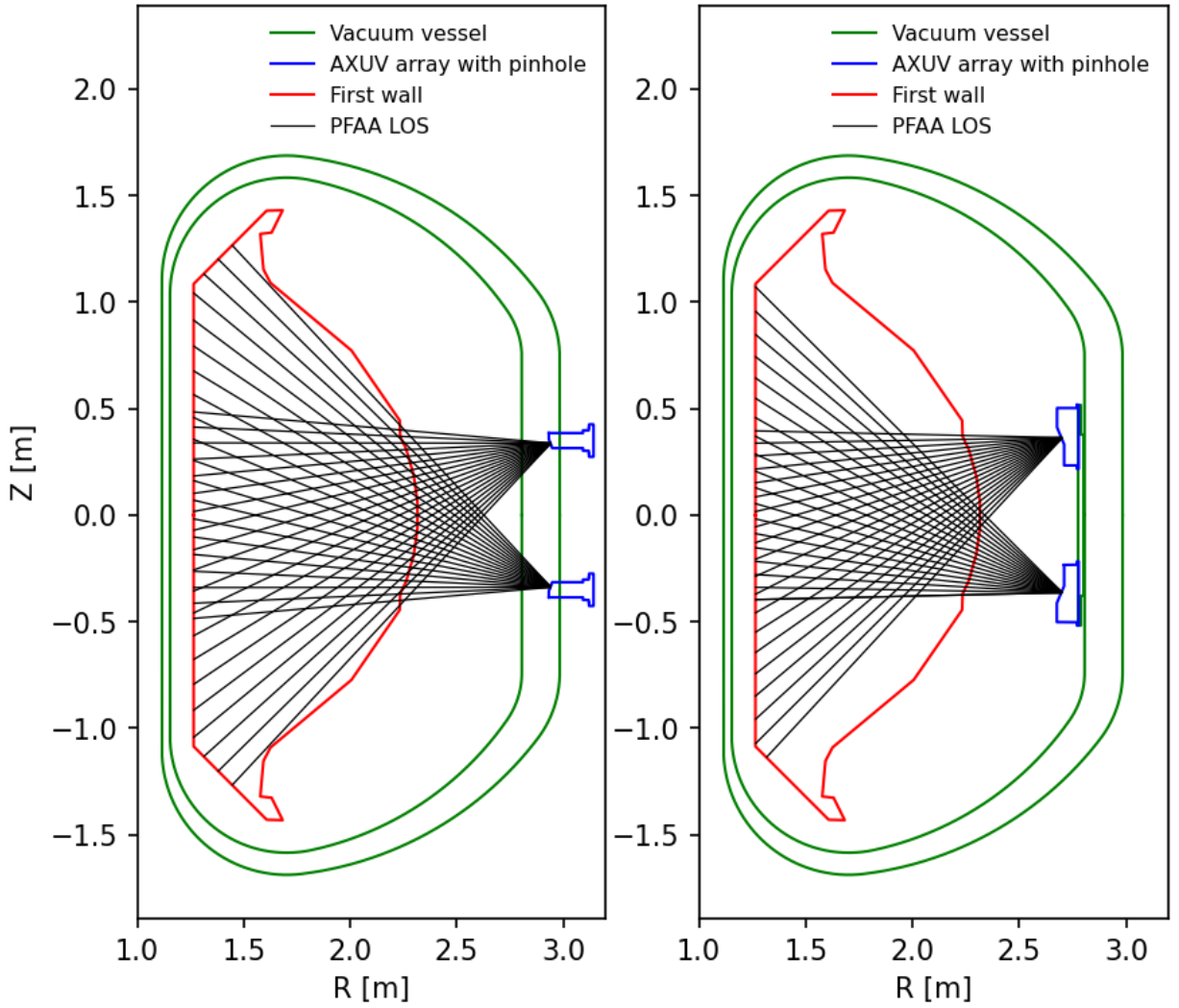

PFAA-D (left) / -O(right) Lines of sight

Introduce Bayesian Inference and Gaussian Process Tomography

- Gaussian process prior

$$p(\bar{f}|\bar{\theta}) = C_2 \times \exp\left[-\frac{1}{2}(\bar{f}-\bar{\mu}_{prior})^T \bar{\bar{\Sigma}}_{prior}^{-1}(\bar{f}-\bar{\mu}_{prior})\right]$$

- Likelihood of the model: $\bar{d} = \bar{\bar{W}} \cdot \bar{f} + \bar{\epsilon}$

$$p(\bar{d}|\bar{f}) = C_1 \times \exp\left[-\frac{1}{2}(\bar{\bar{W}}\bar{f}-\bar{d}_{meas})^T \bar{\bar{\Sigma}}_d^{-1}(\bar{\bar{W}}\bar{f}-\bar{d}_{meas})\right]$$

- Posterior [5]

$$\bar{\mu}_{post} = \bar{\mu}_{prior} + \left(\bar{\bar{W}}^T\bar{\bar{\Sigma}}_d^{-1}\bar{\bar{W}} + \bar{\bar{\Sigma}}_{prior}^{-1}\right)\bar{\bar{W}}^T\bar{\bar{\Sigma}}_d^{-1}\left(\bar{d}_{meas} - \bar{\bar{W}}\bar{\mu}_{prior}\right)$$

$$\bar{\bar{\Sigma}}_{post} = \left(\bar{\bar{W}}^T\bar{\bar{\Sigma}}_d^{-1}\bar{\bar{W}} + \bar{\bar{\Sigma}}_{prior}^{-1}\right)^{-1}$$

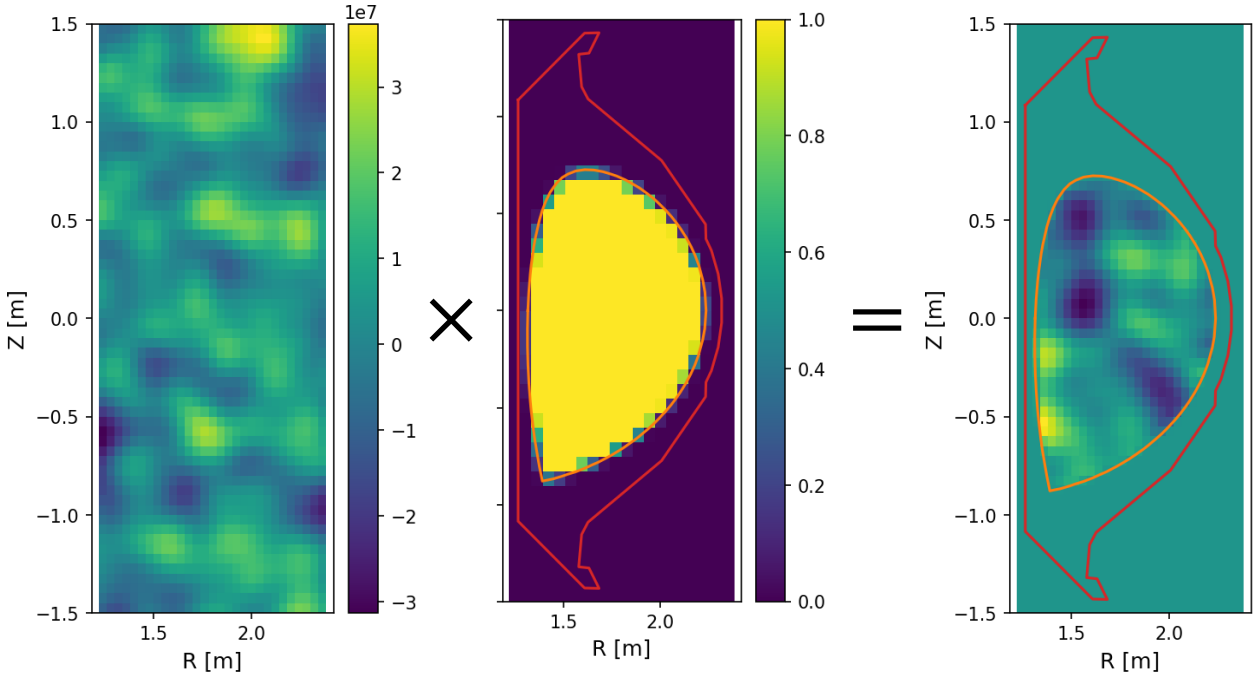

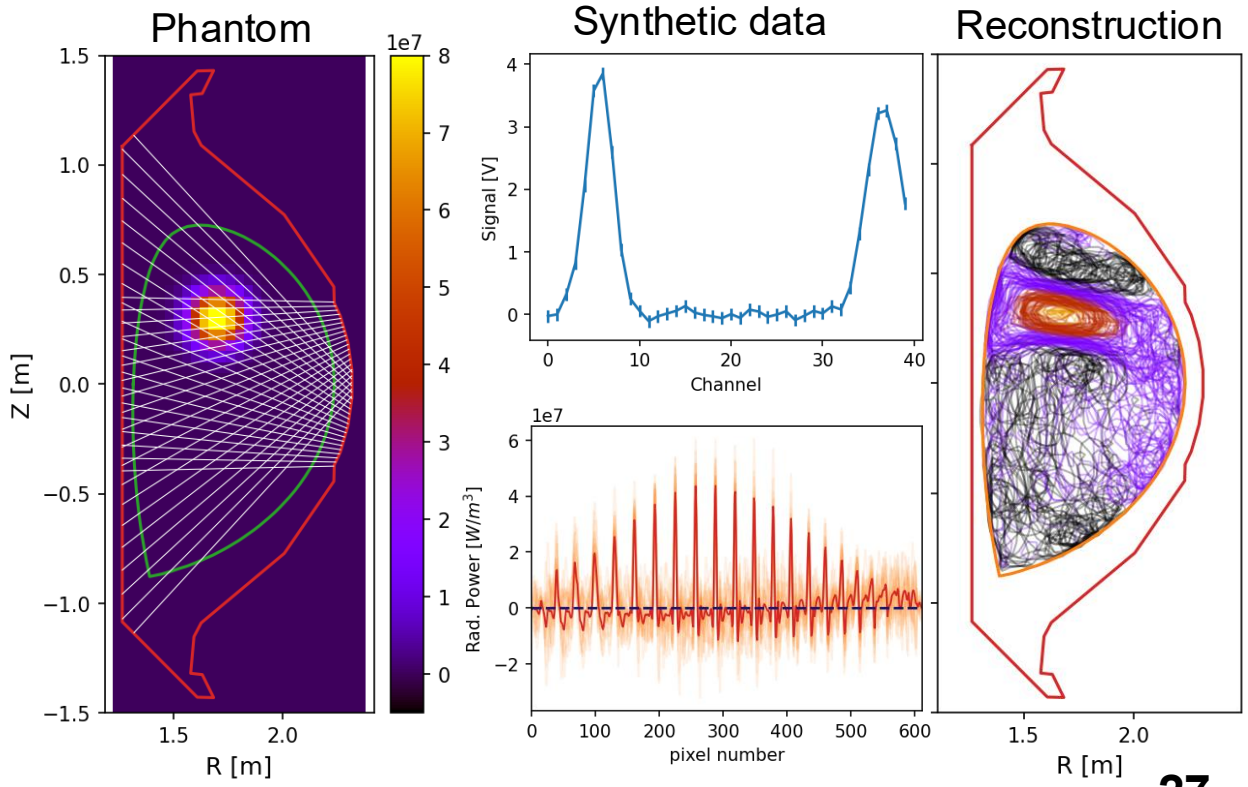

Negative emission makes several problems for tomography reconstruction

- Without absorption, negative radiation in the tomography results is non-physical, but we have negative values
  - -> The total power of radiation is expected to be lower than actual.
  - -> It was not possible to estimate the shape of radiation well.
- Crossing points of two pinhole arrays are sparse along radial direction
- We can not utilize symmetry along flux surface for disruption study.

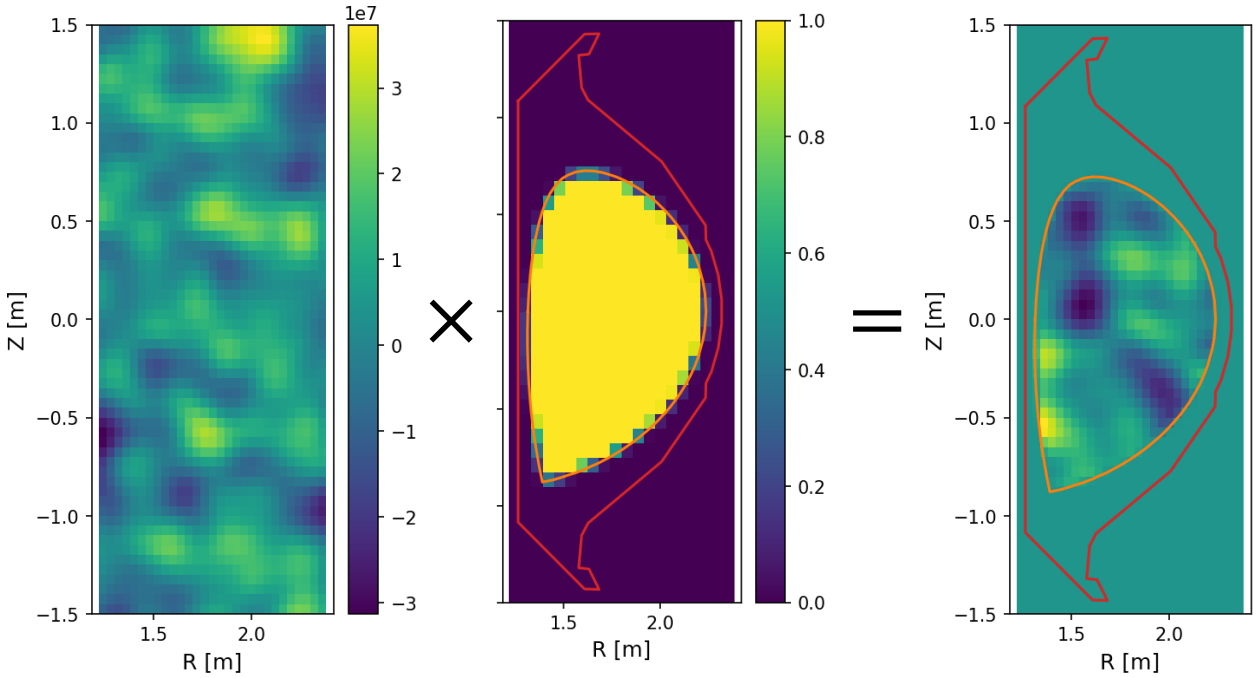

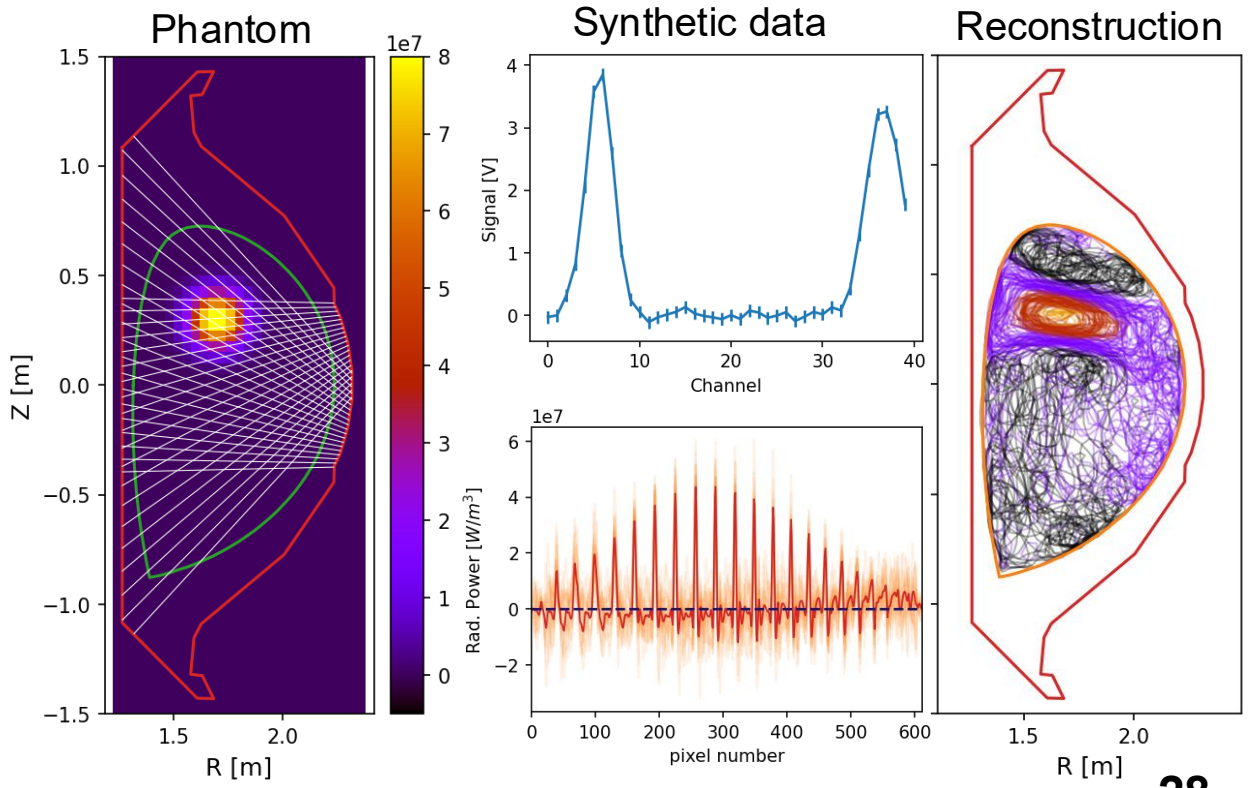

Get samples of Nonnegative Gaussian process tomography through Gibbs sampling

- Monotonically decreasing gaussian process is a kind of TMVN (Truncated Multivariate Normal Distribution)

- $p(\bar{f}|\bar{d},\bar{\theta}) \propto \exp\left(-\frac{1}{2}(\bar{f}-\bar{\mu})^T\Sigma^{-1}(\bar{f}-\bar{\mu})\right)$ for $x \geq 0$,

  0 for otherwise

- Gibbs sampling is a kind of efficient MCMC algorithm which can sample from TMVN distribution [*]

1. Begin with initial value $\bar{X}^i = (x_1^i, x_2^i, \dots, x_n^i)$
2. For next sample, sample from
   $p(x_1^{i+1}|x_2^i, x_3^i, \dots, x_n^i, [\infty, 0])$
   $p(x_2^{i+1}|x_1^{i+1}, x_3^i, \dots, x_n^i, [\infty, 0])$
   $p(x_3^{i+1}|x_1^{i+1}, x_2^{i+1}, \dots, x_n^i, [\infty, 0])$
   …
   $p(x_n^{i+1}|x_2^{i+1}, x_3^{i+1}, \dots, x_{n-1}^{i+1}, [\infty, 0])$
3. For m samples, repeat it m times

Conditional truncated univariated normal distribution with other given values

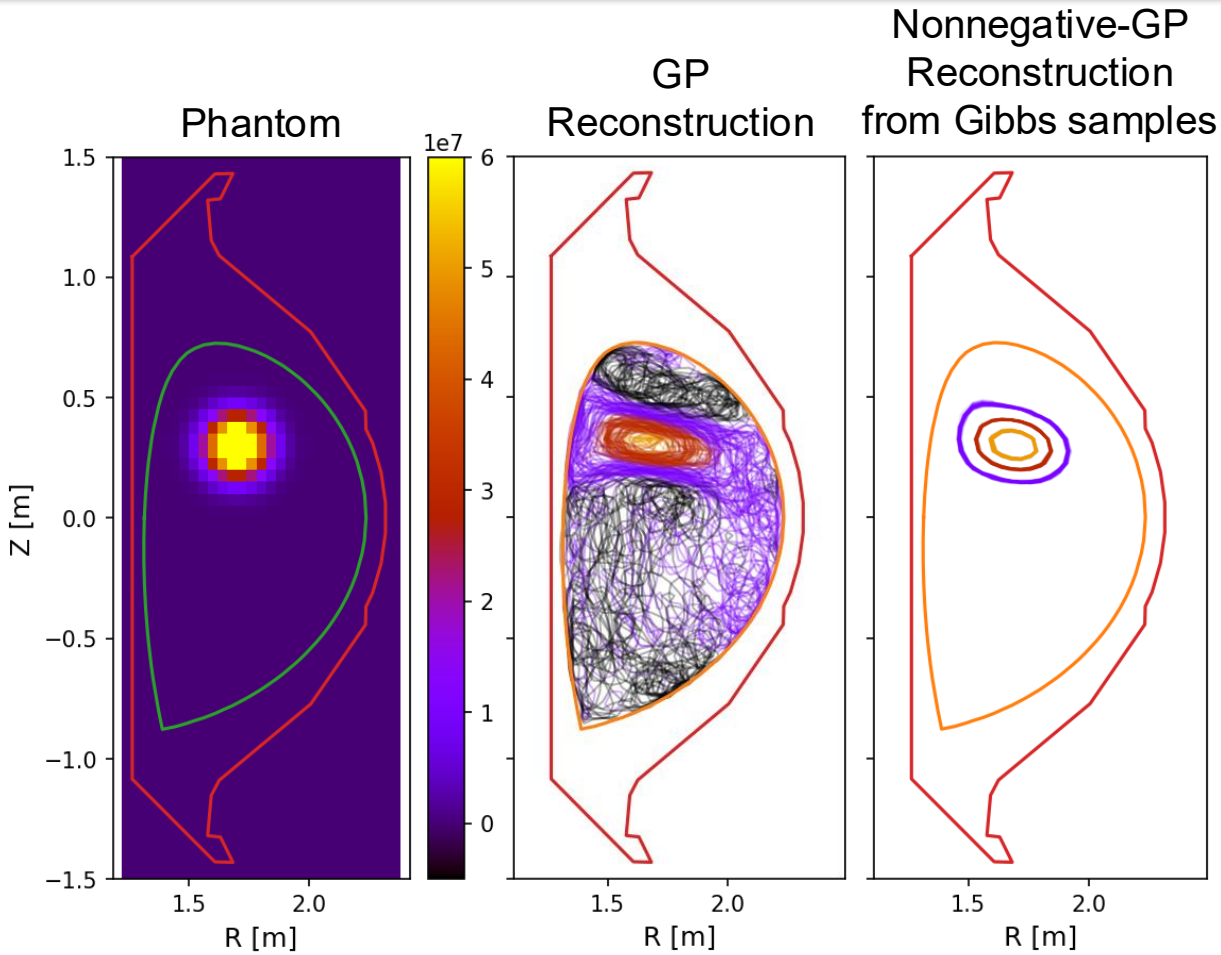

[*] J.A. Breslaw, Applied Mathematics Letters **7**, (2011)

Tomography reconstruction for disruption study in KSTAR is challenging problem - Nonnegative prior can solve this!

- Shattered Pellets are injected at KSTAR O-port and G-port
- Poloidal Filtered AXUV arrays are installed at D-port and O-port
- Each AXUV array system is pinhole array with 20 lines of sight
- Superconductor tokamak has lack of view ports
  - PFAA systems have bad and poor line of sight arrangement

t=4.0028s
GPT w/o constr.

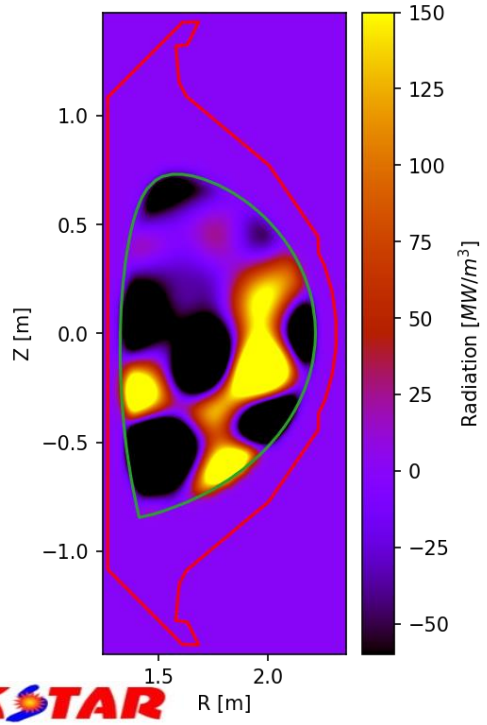

t=4.0028
GPT with Nonneg.

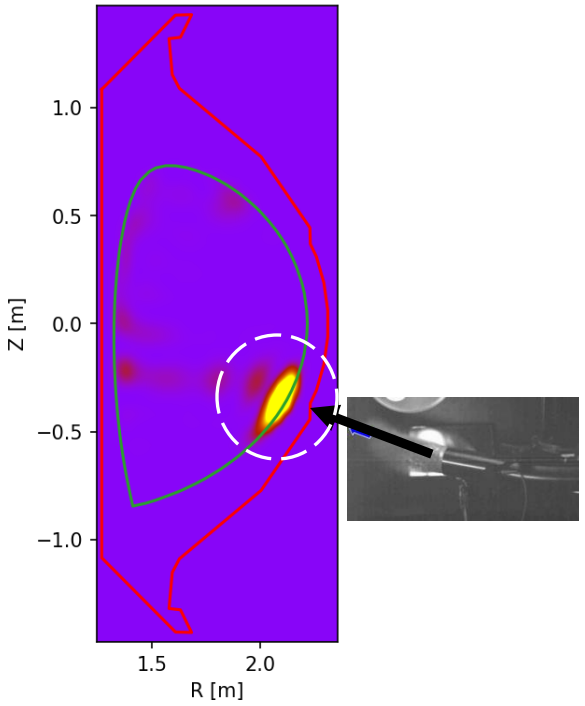

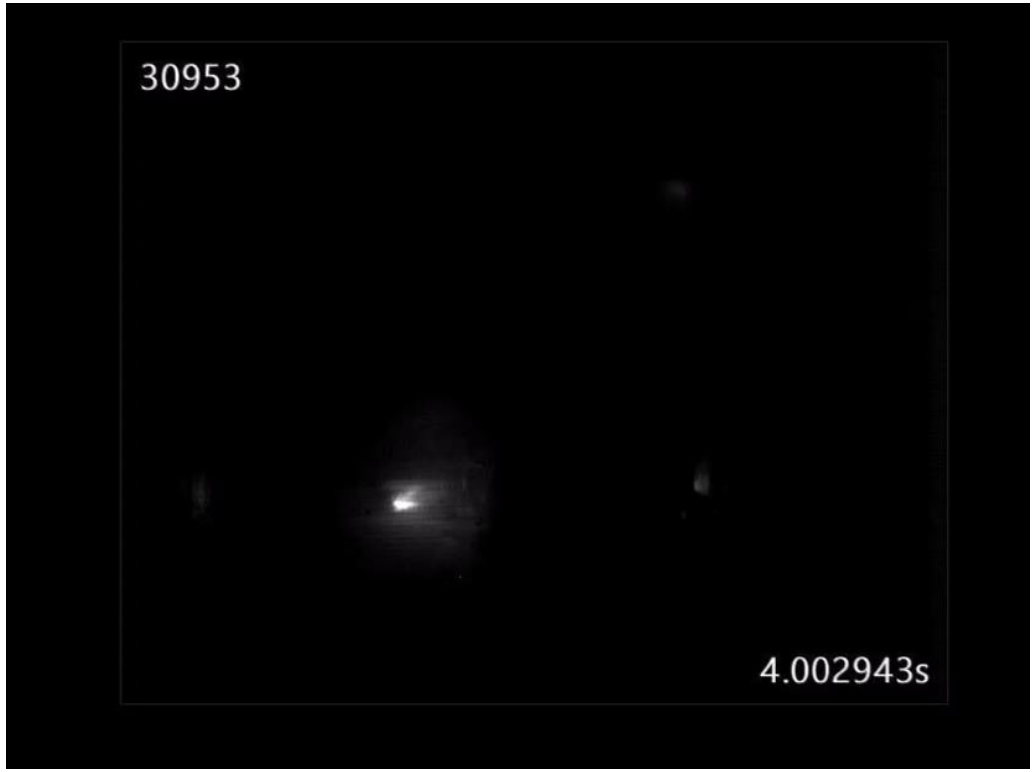

Fast visible camera data indicate plasma radiation have strong asymmetry along poloidally and toroidally during pellet induced disruption

Summary

- Bayesian data analysis can be used for…
  - Data fusion to fully utilize given data and to get more exact plasma parameters
  - It can utilize prior as much as possible to increase data analysis quality
  - Model optimization finds adequate hyperparameters for data analysis
- Adequate diagnostic model provide better result.
- Some KSTAR diagnostic result utilize Bayesian inference
  - We want to expand the use of Bayesian inference for more diagnostics

- Bayesian inference have many other applications… (will be our future work)
  - Data analysis considering outlier
  - Data analysis with neural network (forward model can generate synthetic data)
  - …